Forensic rock mechanics for the analysis of rockbursts and seismicity in mines – Session I

Gerrie van Aswegen

1 Introduction

This two-lecture series is mainly aimed at SA rock mechanics practitioners, but it may be of general interest. I wish to partly share my particular experience and interests – some of it may even be useful

There will be no mathematical stuff. For true seismologists, mathematics is their mother tongue. I am just a geologist with experience in mine seismology, or, as I think it should be called, dynamic rock mechanics.

- Session I will not cover seismology at all and the focus is on some basic principles of rock deformation and failure. It is kindergarten stuff, but useful to establish nomenclature and the concept of a sequence of events. Preparing these notes I got carried away a bit by extension fracturing, fractography, shatter cones and pseudotachylites, but all the time mindful of the fact that all these phenomena (apart from the shatter cones) are observable in our gold mines.
- Session kicks off with some very basic seismology and then I continue with a series of case histories to show how to combine seismology (source parameters, source mechanisms) with detailed underground observations and a basic understanding of rock mechanics to unravel “what happened”. In the process I attempt to bring some clarity and simplification to the concept of seismic moment tensor as applied in mines. Once you understand “what happened”, you can figure out what went wrong and take steps to avoid recurrence.... although we learn from history that we do not really learn from history

Note that there is nothing new here. The lectures are based on published papers and I have presented most of the material several times/places before.

2 Scale invariance

I want to first refresh our memories about the concept of scale invariance. It is reflected by the power law distribution of seismic event sizes which forms the basis for seismic hazard assessment – not a subject of discussion here!

I raise the issue of scale invariance since, together with variations in rock properties, it may help to explain some apparently anomalous stress patterns – considered at the end of this Session.

In rock mechanics the concept of scale invariance may be used to define artificial rock masses for stress modelling. The idea is that the same structure/pattern is repeated many times at different scales according to a power law.

An example of scale invariance in fracture patterns is given in Figure 1. We also see a series of extension fractures forming subsets at different scales (Figure 2 and Figure 3).

We may note that natural fractures and faults do not follow power law distributions perfectly (Figure 1). One general reason being that rock properties are not scale invariant, e.g. the shear modulus may depend on the sample size.

We revisit scale invariance at the end of this Session when I try to explain particular stress anomalies.

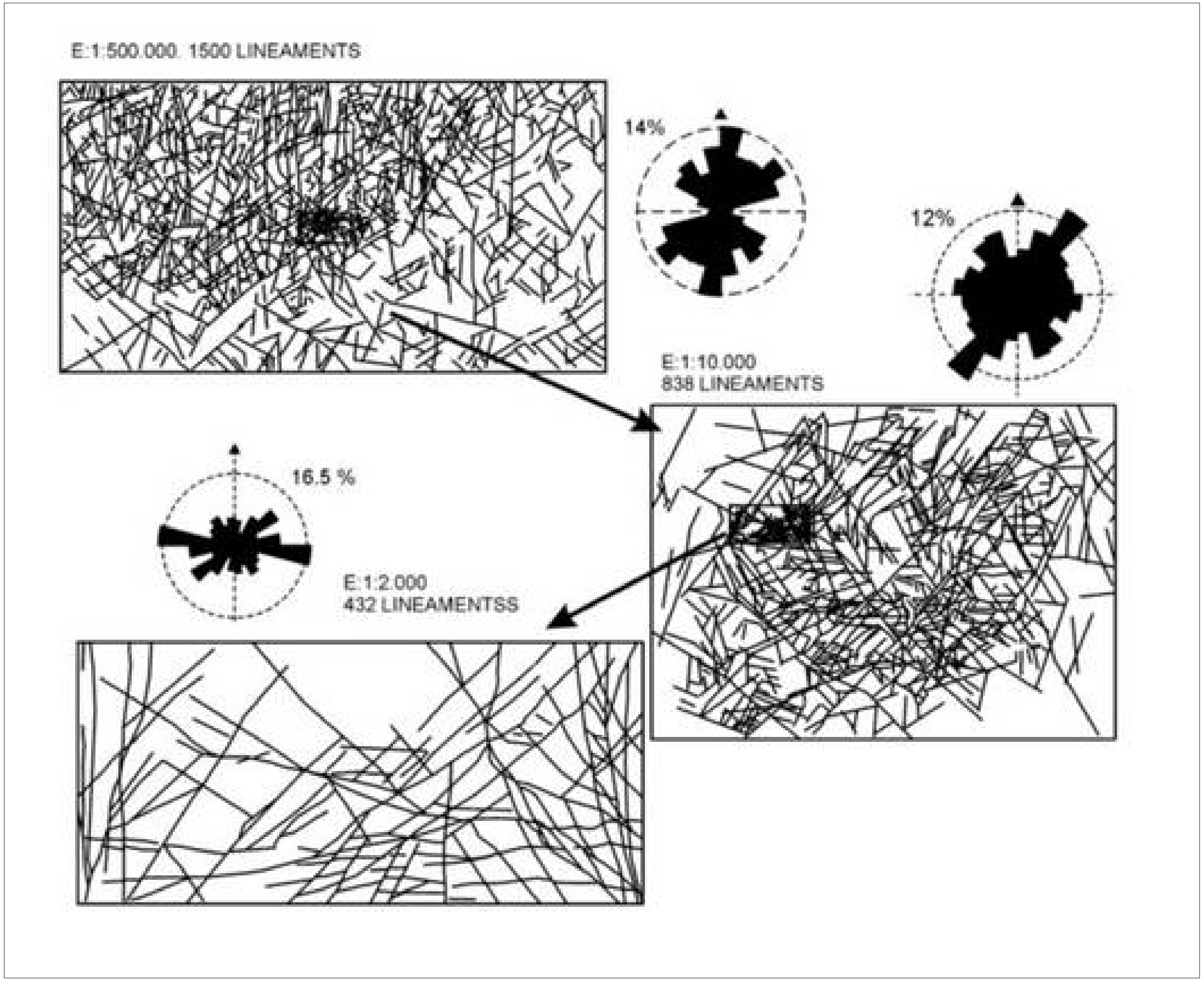

Figure 1: Morphological lineaments interpreted from digital elevation models (DEM)*. (Pérez-López* et al., 2005)

Figure 2: Raaswater brittle shear zone.

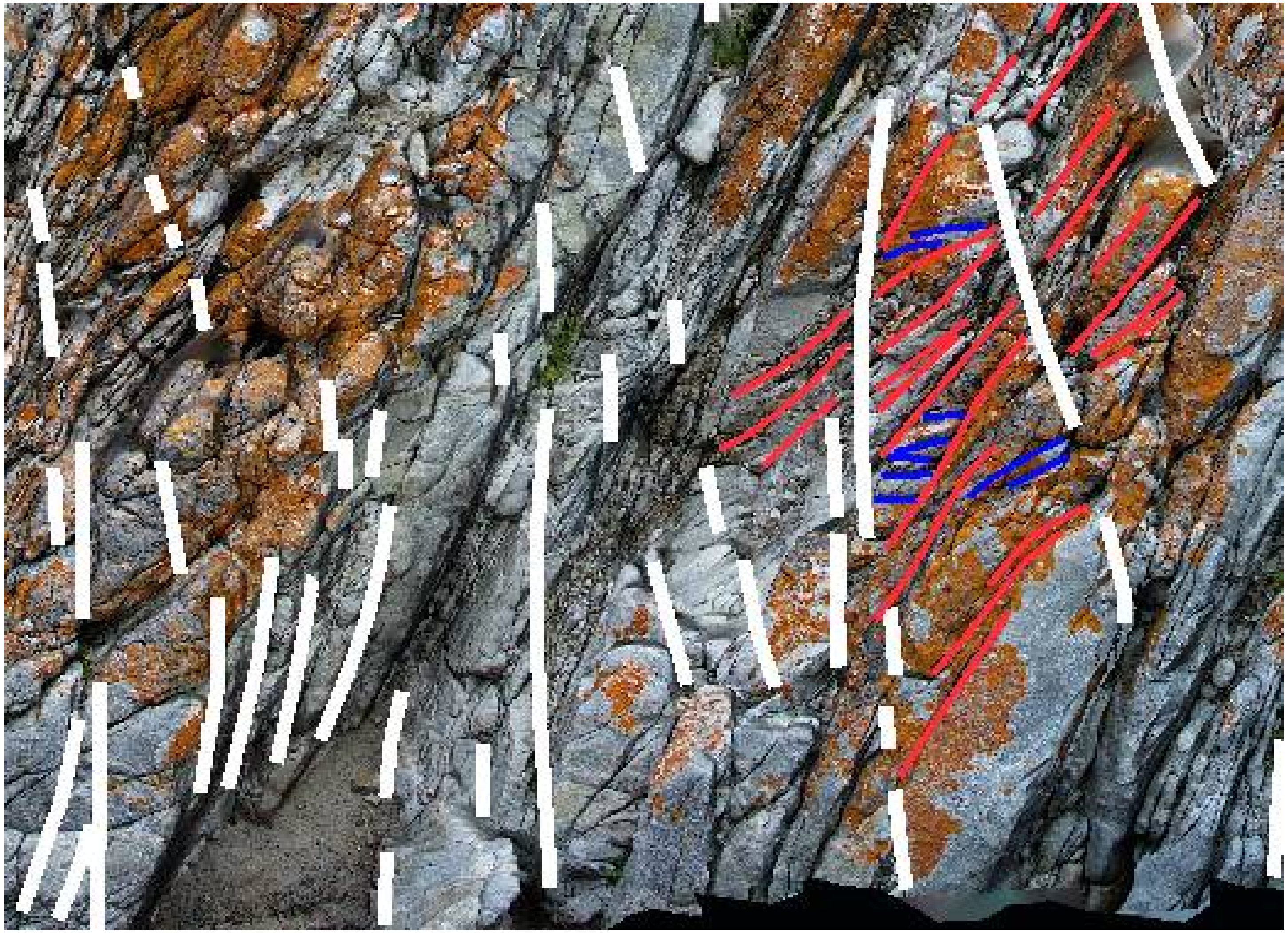

Figure 3: Zoomed in on part of the above. The main fracture zone (f1) is followed by a set of sub-fractures (f2 – white) joining the main fracture zone asymptotically. Between f2 fractures a third subset is evident (f3- red) and, at one place at least, a fourth subset (f4 - blue).

3 Some simple rules about rock deformation and failure

Here I refer to very basic rock mechanics, some terminology (and a particularly irksome and erroneous use of the term "pure shear") and the relation between stress orientation and fractures. In general (Figure 4):

1. Because simple shear yields volume constant plane strain and because rock has limited compressibility, rock tends to deform in shear – it is simply the easiest way for rock to deform.
2. Because rock is weakest in tension, it tends to fail in tension.
3. Extension fractures develop normal to δ_3 while shear fractures at ~30° to δ_1
    - Anderson's classification (Figure 5)
4. The higher the strain rate, the smaller the fragments of rock at failure – leading to rock flour in the case of highly dynamic deformation. This we revisit in Session II

These simple 'rules' largely determine the evolution of extension fractures, shears and comminuted rock material commonly observed in the deep gold mines of South Africa.

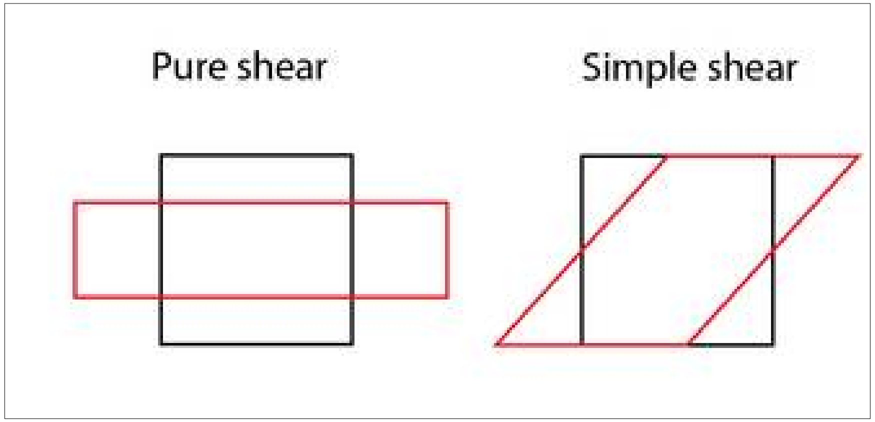

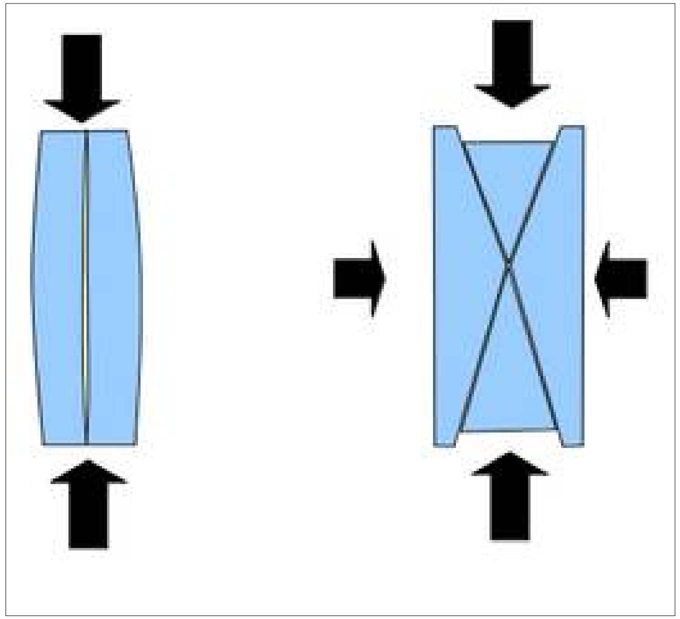

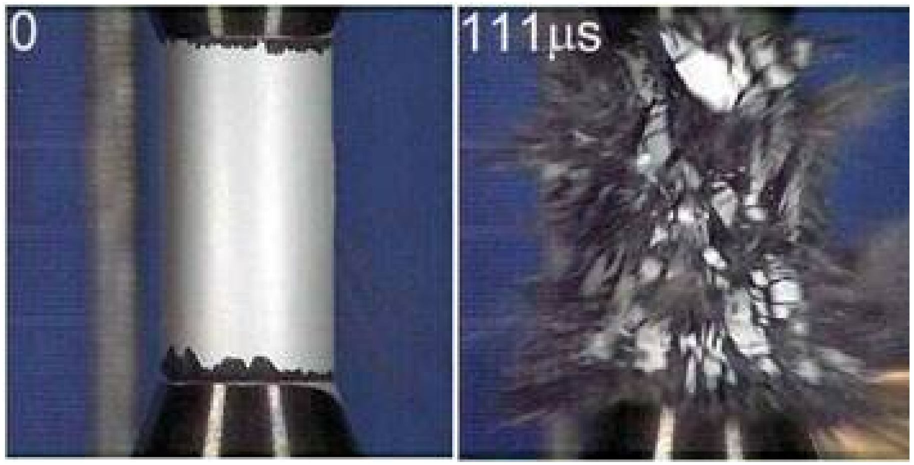

Figure 4: Self-explanatory pictures depicting pure shear vs simple shear, uni-axial vs triaxial deformation and high failure rate. Note that pure shear ≠ simple shear

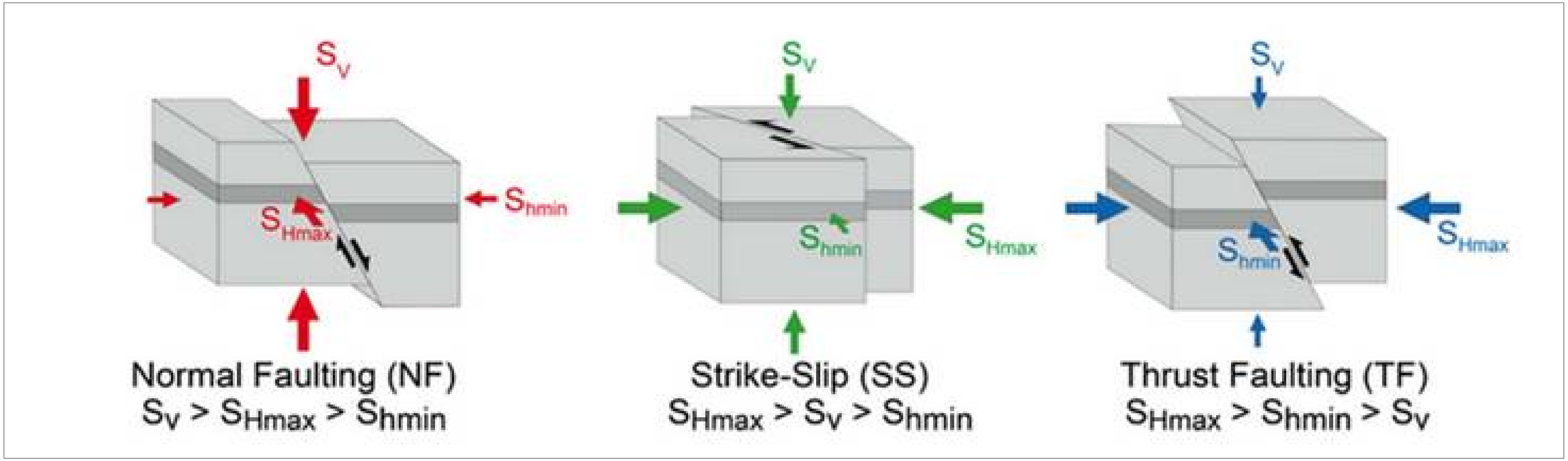

Figure 5: Andersonian faults

4 Extension fractures

4.1 Definition

Extension fractures, also referred to as a "dilatant cracks" (e.g. Pollard et al., 1982) are extremely common geological structures, mostly seen as joints. Joints are the most common geological fracture structure. Much of geotechnical engineering is about controlling rock deformation along joints.

Most natural joints are extension fractures caused by tectonic load – only down to ~12 km – deeper than that most rocks yield in a ductile fashion. Cooling joints form spectacular outcrops and apparently can form at great depths.

Not all natural extension fractures are joints of course, geologists will argue about when a fractures should be called a joint and when not (Figure 6).

An extension fracture forms when the extension strain exceeds the rock specific critical value of extension strain, as described by Dick Stacey (1981):

"*The criterion is extremely simple in concept and is summarized as follows: Fracture initiates when* $e >= e_c$ *where* e_c *is a critical value of extension strain for the rock. The resulting extension fractures always lie in the plane normal to the orientations of the least compressive principal stress. The fractures will form in planes normal to the direction of the extension strain, which corresponds with the direction of the minimum principal stress. For a material which shows ideal linear deformation behaviour, the strain in this direction is related to the three principal stresses by the following equation:*

$$\varepsilon 3 = 1/E[\delta_3 - \nu(\delta_1 + \delta_2)],$$

where δ_1, δ_2,δ_3 *are the principal stresses, E is the modulus of elasticity, ν is Poison's ratio. From this it can be seen that, if* $\nu(\delta_1 + \delta_2) > \delta_3$, *then an extension strain will occur.*

Note thus that extension fractures can form when all three principal stresses are compressive

Figure 6: Drone view of intense extension fracturing of TMS at de Kelders

4.2 Gradation from extension fracture to shear fracture.

We further note that, like for many natural phenomena, there is a continuous transition between extension fractures and shear fractures (Figure 7).

We can also see such gradations in our mines. A case in point is the site of a rockburst in the Postma dyke, WH3#, in the early nineties. I had the opportunity to crawl into damaged advanced strike gulley (asg) which they develop ~halfway through the ~20m thick dyke. The deeper part of the asg was closed during the rockburst, but the first metre or two were opened as part of the rescue operations. At the entrance to the asg, the usual face-parallel extension fractures were evident. A couple of figures show parallel extension fractures at the face and an increased angle between conjugate sets of fractures as the distance ahead of the face increases. (Figure 8 to Figure 11). About 50cm in, a set of conjugate fractures at an angle of ~13° was visible (Figure 10) and 30 cm further in, another set showed an angle of 23° (Figure 11). The conjugate sets indicated an anomalous face-parallel but sub-horizontal direction of compression, i.e. not normal to reef as expected. The reason for the particular orientation of stress is unclear.

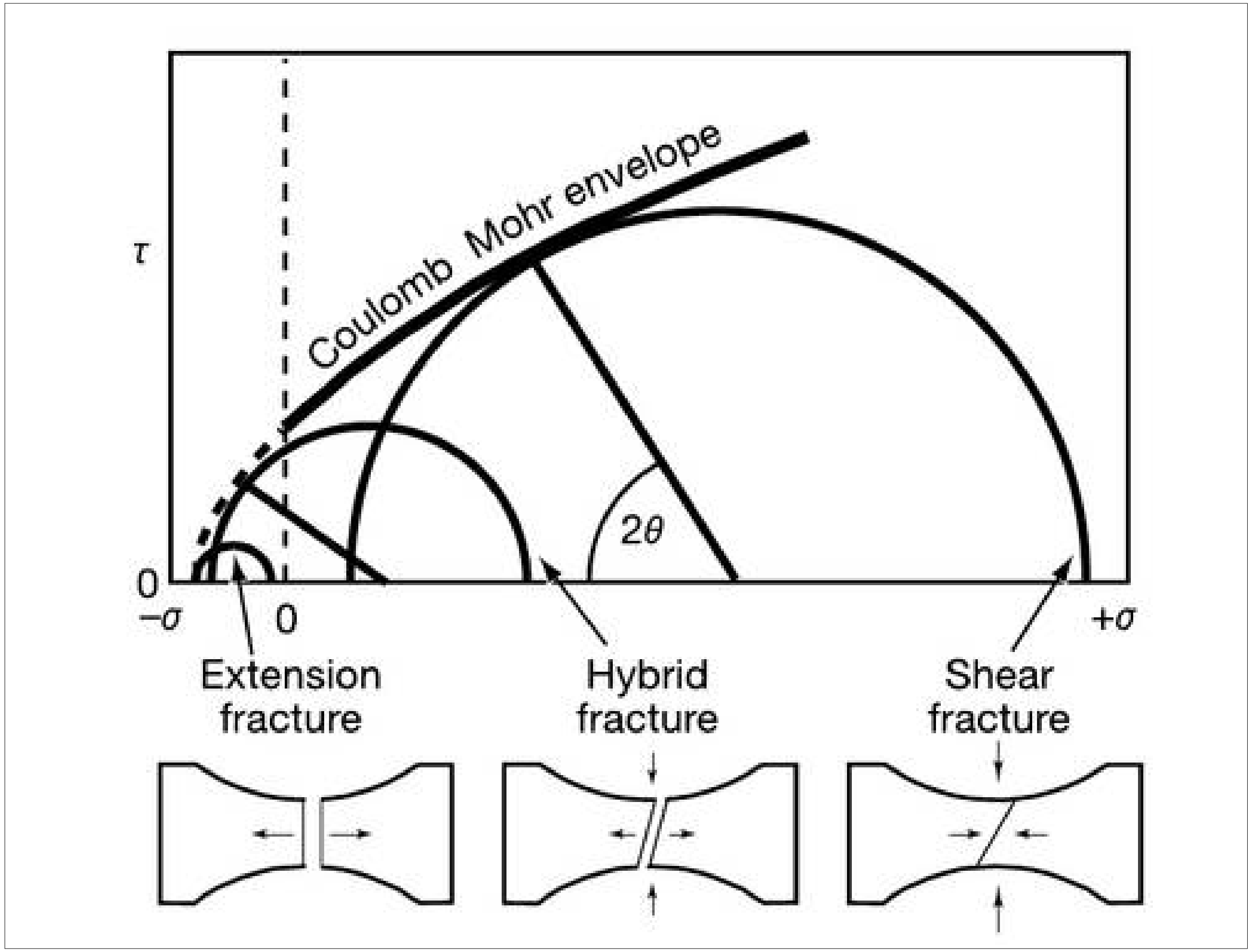

Figure 7: Transition from extension fracture to shear fractures is continuous (Ramsey, J.M. and Chester, F.M. (2004).

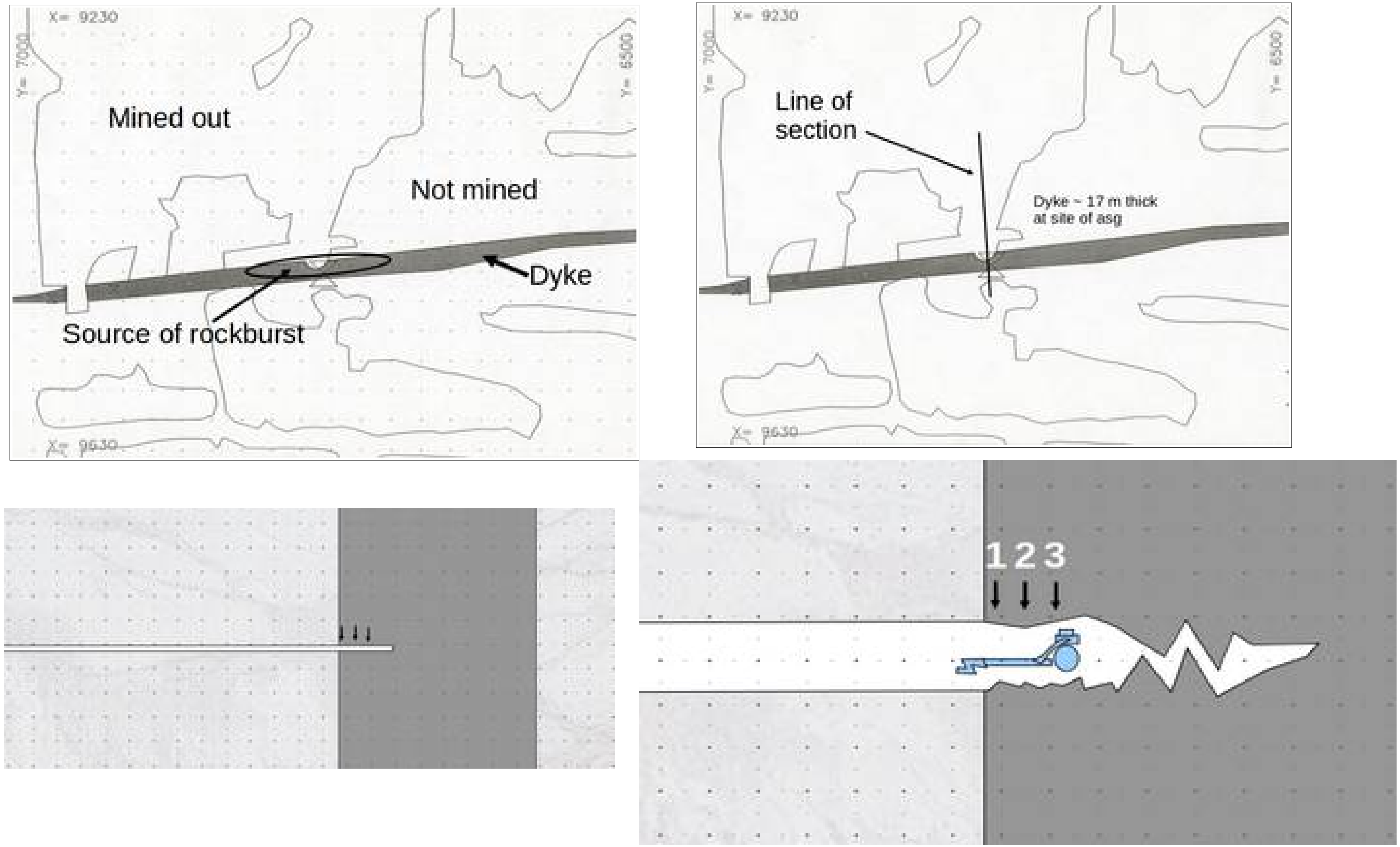

Figure 8: Plan and schematic section views of the site of a rockburst on the Postma dyke. The numbered arrows in the section view refers to the photographs on the next pages.

Figure 9: Fractures at position 1 in the section shown in Figure 8

Figure 10: Fractures at position 2 in the section shown in Figure 8

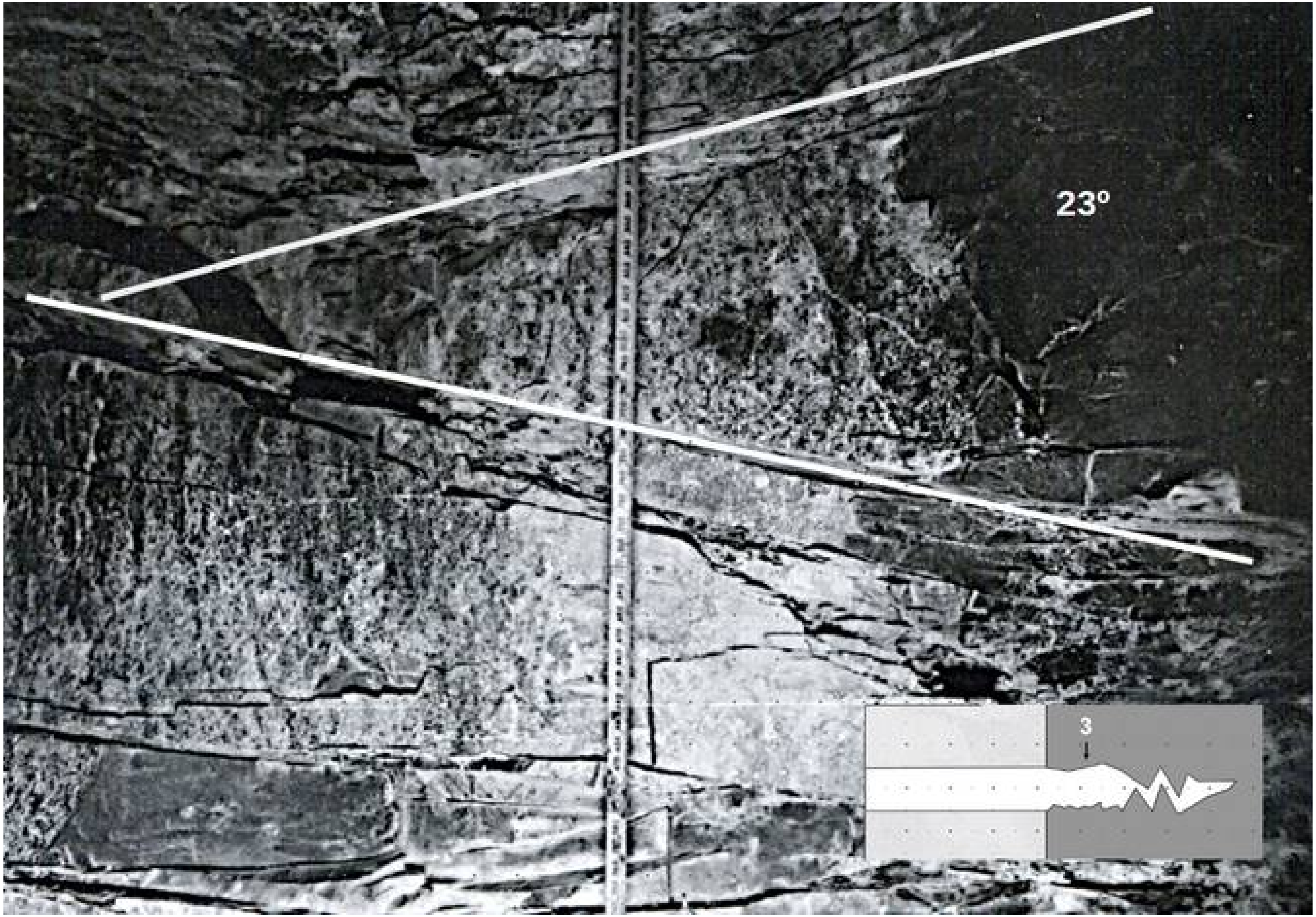

Figure 11: Fractures at position 3 in the section shown in Figure 8

4.3 Extension fractures are fossil traces of stress trajectories

We note that, by definition, an extension fracture reflects the stress orientation at the time of the development of the fracture. The stress orientation may change later on (minutes, hours, years, millions of years later) and the fracture thus remains as a fossil trace of the original stress trajectory.

Ahead of a stope or a tunnel, the stress continuously changes from blast to blast. In that way, a set of extension fractures ahead of the face quickly finds itself in a stress environment conducive to shear (Figure 12).

As an aside, we note that unravelling the sequence of deformation events is one of the aims of structural geological analysis. We also try to establish the sequence of deformation events when we do “forensic rock mechanics”. While the sequence may be obvious in places (Figure 27), the exact timing of the different events could be impossible to establish.

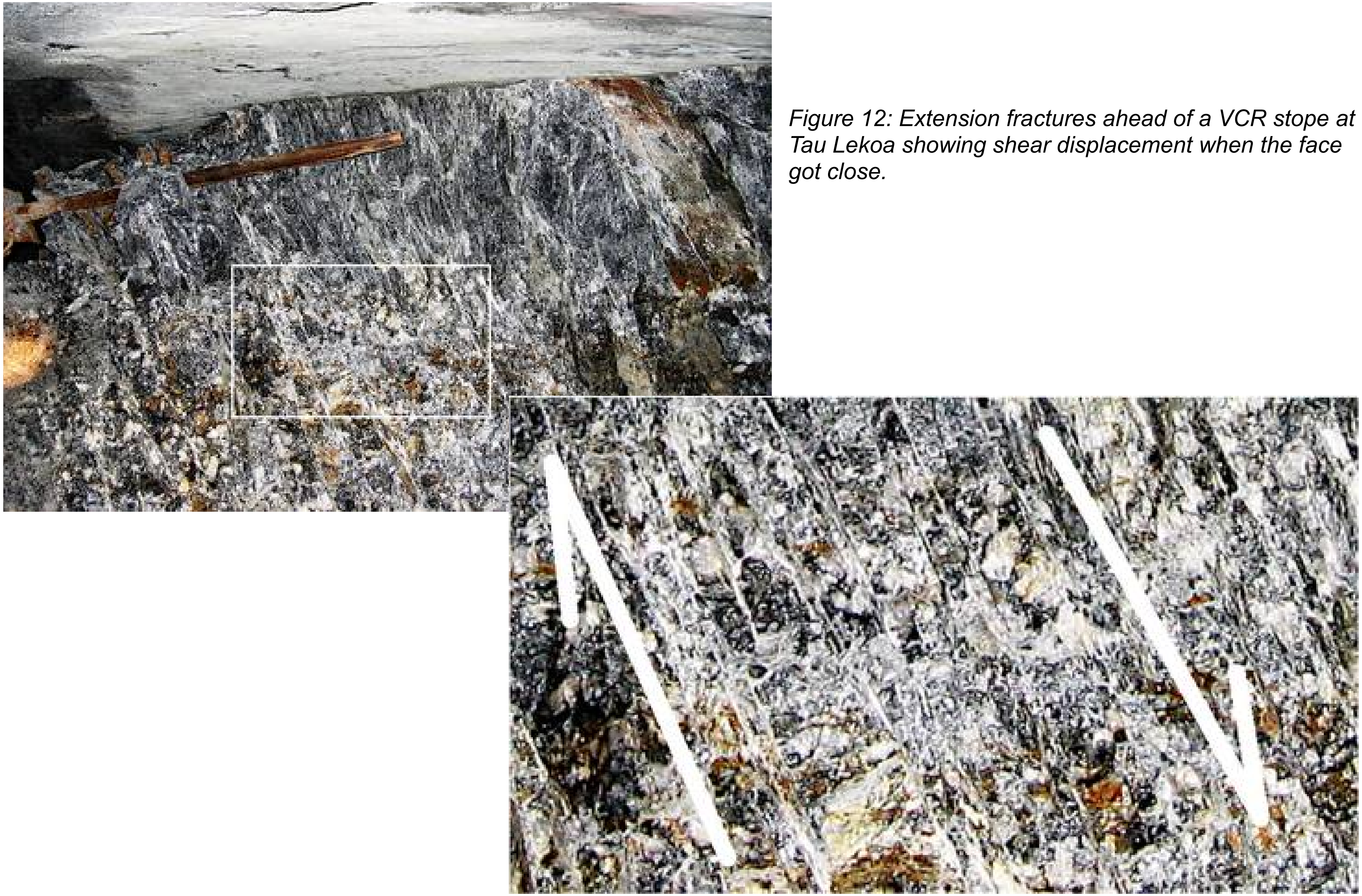

Figure 12: Extension fractures ahead of a VCR stope at Tau Lekoa showing shear displacement when the face got close.

4.4 Dynamic and kinematic indicators along extension fractures.

4.4.1 Dynamic vs kinematic

We note that, because rock is weak in tension and because extension fractures develop in the brittle domain, the crack usually forms very fast. Since the crack propagation starts at a velocity of zero and can reach the velocity of the Raleigh-wave, they are dynamic features (remember the classification static [m], kinematic [m/s] and dynamic [m/s^2])

4.4.2 Slickensides (kinematic)

Along faults, the best known kinematic indicator is slip striations or slickensides (see below). We consider this in some detail in Session II.

Since the extension fracture develops normal to δ_3, which is a plane of zero shear stress, it is not possible for slip striations to develop along it during the (dynamic) event of fracture formation. However, some time later, some change in stress orientation may occur, allowing shear stress and slip along the fracture.

4.4.3 Fractographic striations (mostly dynamic)

We note on many a fracture surface a particular kind of striation which geologists refer to as “plumose” structures. Fractography is the art of qualitatively interpreting the mechanisms of fracture that occur in a specimen by microscopic examination of fracture surface morphology. https://www.sciencedirect.com/topics/materials-science/fractography

Where fractography is applied on geological scale, it is referred to as tectonofractography (e.g. Bahat et al., 2012).

In our mines we are somewhere in between these extremities.

Dave Ortlepp was maybe the first to study these structures in SA mines (Figure 13, Figure 14). We often see these features in road cuttings where fractures were formed during blasting and also in the natural environment (Figure 15 to Figure 17).

Although not all researchers agree on specifics, a working nomenclature has developed to describe the fractographic features (Figure 18, Figure 19). Note the concept of “plumose axis”, generally considered to be parallel to δ_1. Thus it may be possible that slickensides evolve parallel to the plumose axis once the extension fracture has undergone a slight rotation relative to δ_1, both then reflecting the stress orientation during and (soon) after fracturing.

There is some uncertainty about the velocity of rupture propagation in some natural cases and “arrest marks” suggest temporary stoppages. Whether the duration of the “stoppages” are milliseconds or years are unclear. The final phase, where the fracture ends a series of en-echelon cracks is interpreted as the zone along which the rupture velocity reaches a peak and the fracture splits into many to dissipate excess energy (Figure 20).

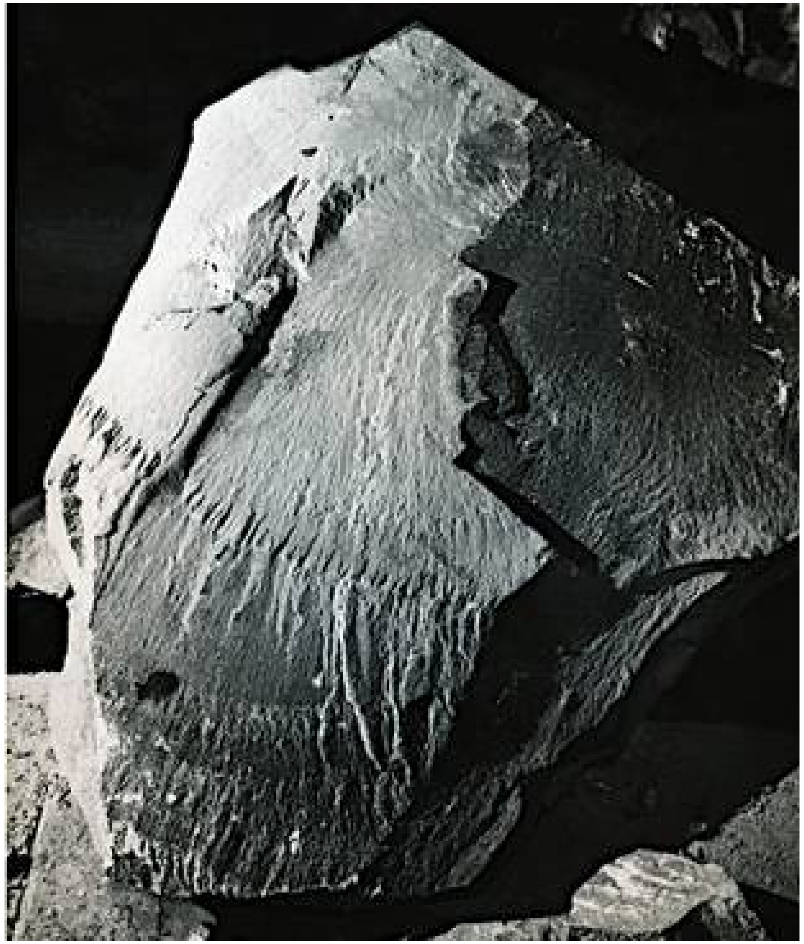

Figure 13: Slab of rock from a strain-burst in a tunnel 90 below a large strike stabilising pillar that suffered 'foundation failure' which generated a large seismic (Ortlepp, 1997)

Figure 14: Buckling of the roof in a shallow coal mine (Ortlepp, 1997)..

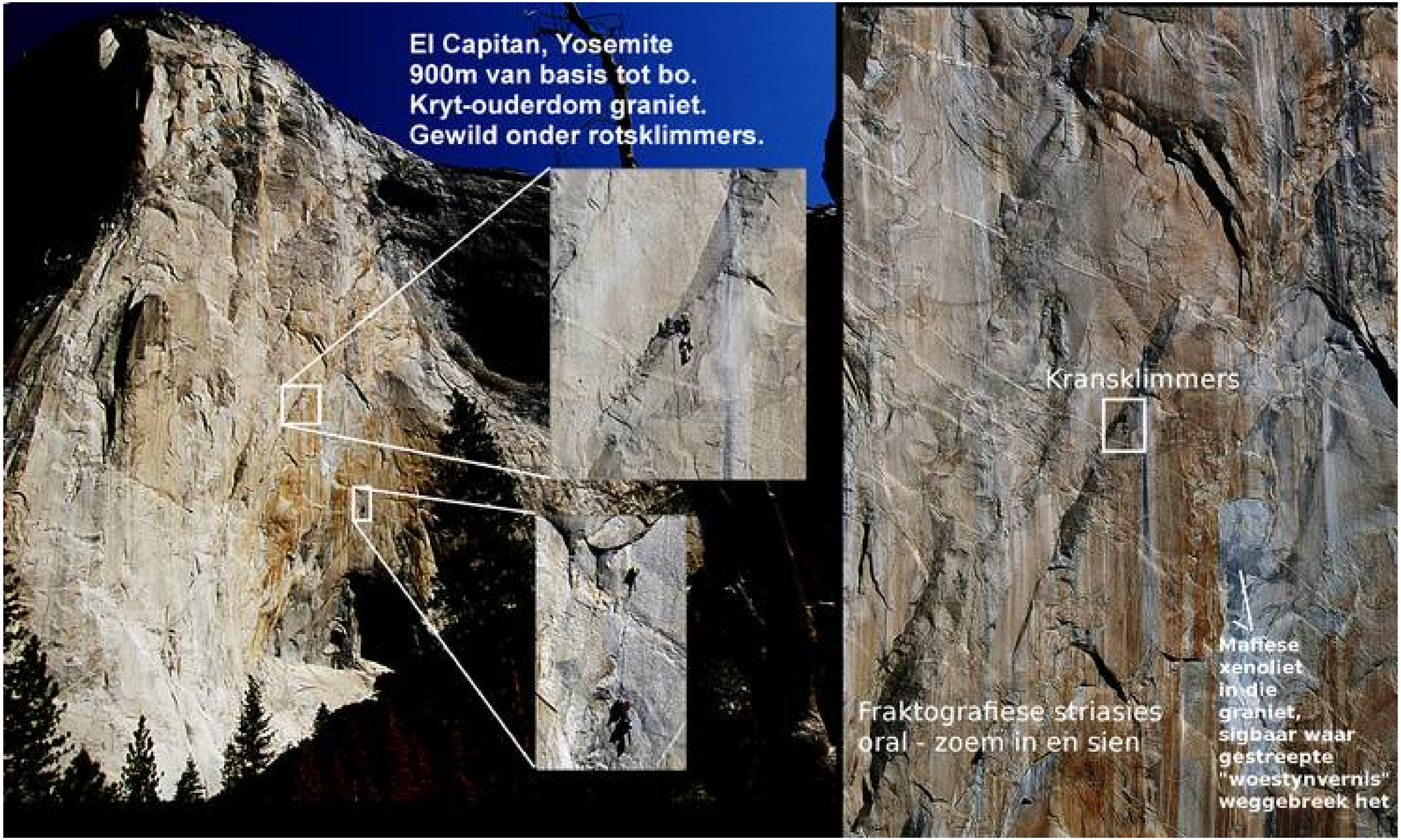

Figure 15: Fractography in Yosemite.

Figure 16: Fractography in Yosemite.

Figure 17: Natural fractographic striae along a fracture in the Cape fold belt

M. Ziegler et al. / Tectonophysics 626 (2014) 1–20 3

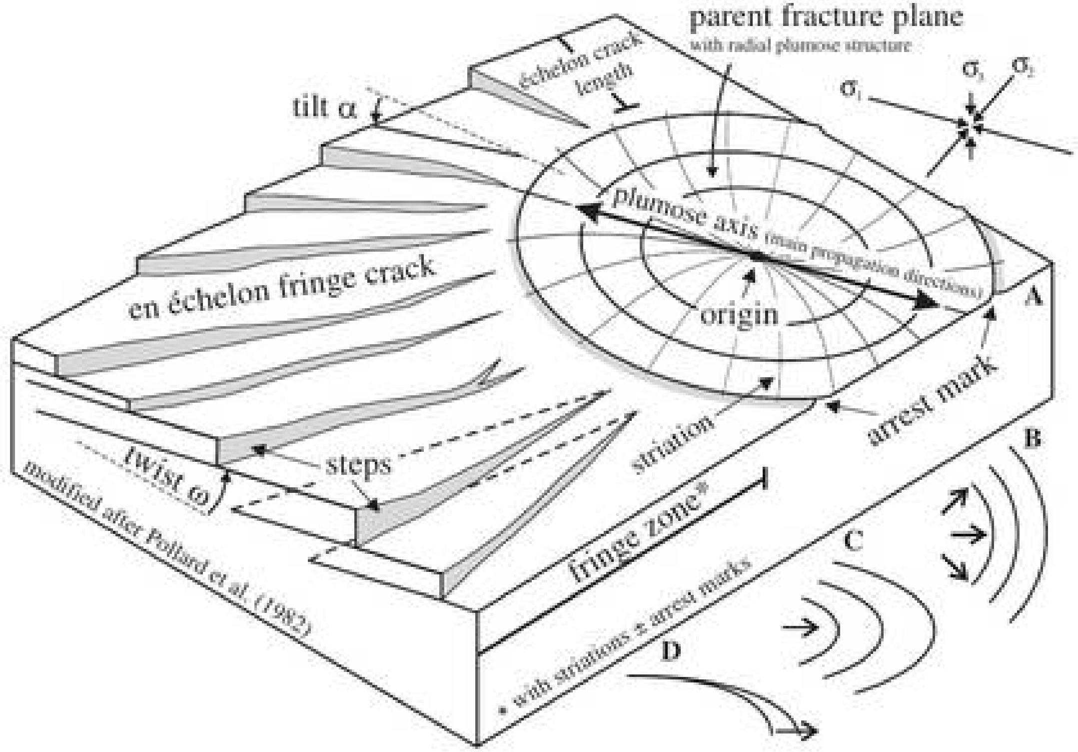

Fig. 1. Sketch (A) of fractographic features frequently encountered on exfoliation fractures in the Grimsel study area: (i) fracture origin; (ii) arrest marks (a subtype of ripple marks); (iii) plumose structure with (iv) plume axis indicating main propagation directions on the parent fracture plane, typically surrounded by (v) gradually-developing en échelon fringe cracks (here with consistently clockwise twist sense, as seen in direction of fracture propagation). Arrest marks can occur in form of concentric (B) or parabolic/elliptical furrows or ridges (C). In places renewed fracture propagation only occurs along parts of existing fracture front lines (D).

Figure 18: Fractography terminology

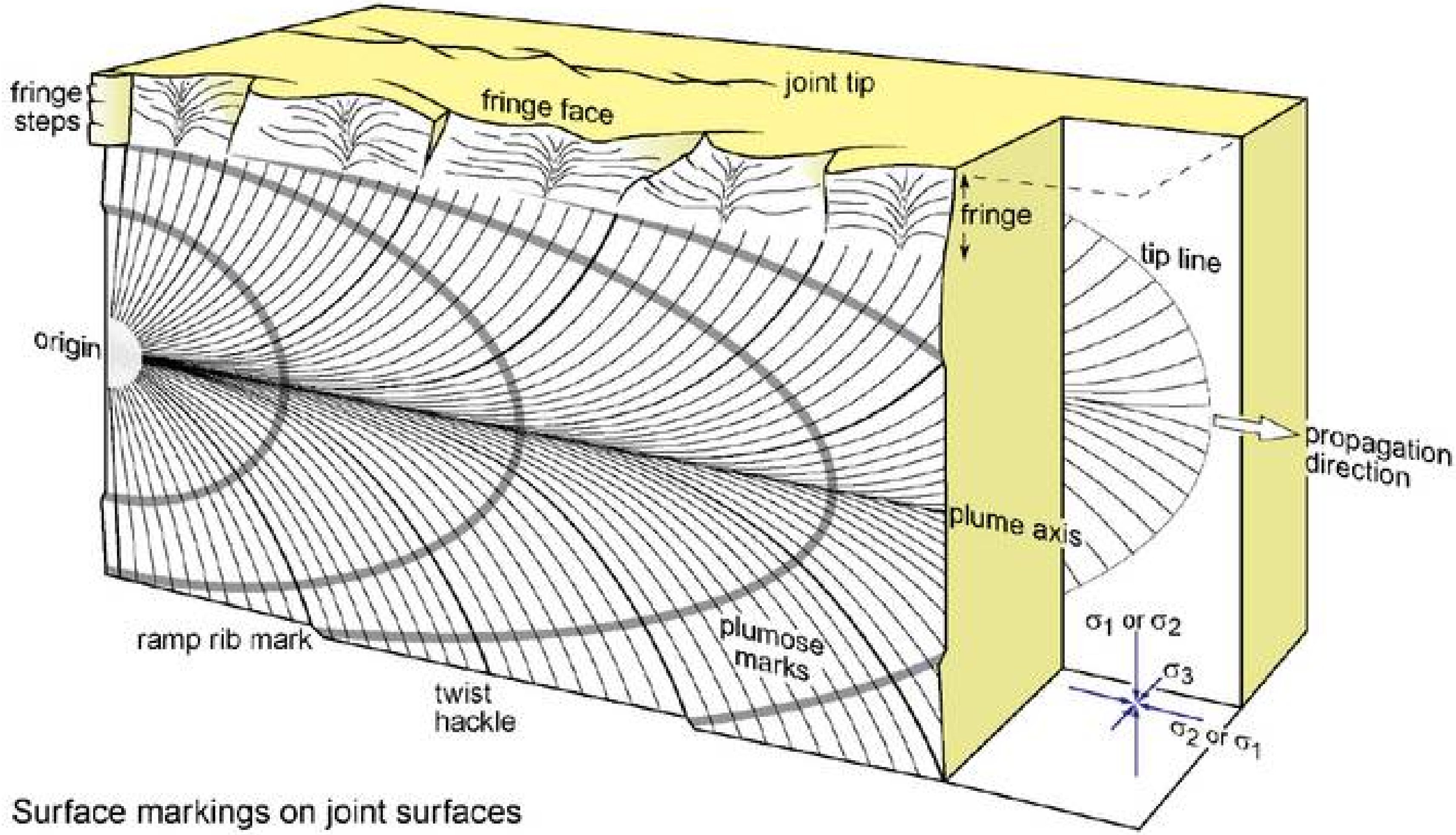

Figure 19: Fractography terminology.

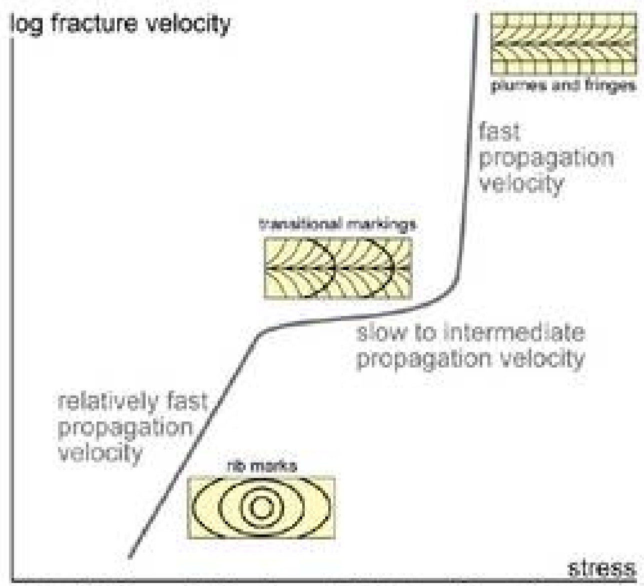

Qualitative distribution of joint surface features
with respect to stress intensity and fracture propagation velocity
(adapted from Weinberger & Bahat, *Terra Nova* 2008, **20**(1), 68-73)

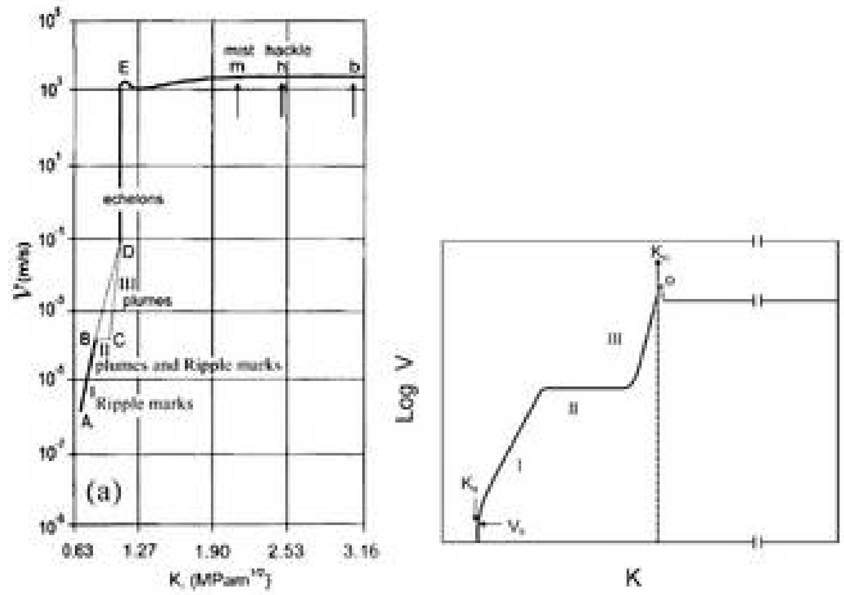

Fig. 6: (left) V versus K_I diagram for pre-uplift joints in granite from the South Bohemian Pluton, synthesized from laboratory experiments (from Bahat et al. 2003). (right) Schematic variation of stress intensity factor (K) with crack velocity (v). K_0: stress corrosion limit, v_0: velocity at stress corrosion limit, K_{Ic}: mode I critical stress intensity factor, I/II/III: distinct regions (from Bahat et al. 2003, and references therein).

Figure 20: Velocity of fracture propagation

4.5 Shatter cones

Shatter cones, as you find around the Vredefort impact structure and other such impact craters, are fractographic features. They reflect the penetrative fracturing of the rock under dynamic load (Figure 21). The Vredefort impact is modelled to have resulted from a body, 10 km in diameter, hitting the earth at 20 km/s, resulting in dynamic fracturing over a wide area. Shatter cones have been recorded up to 60 km away from the dome centre.

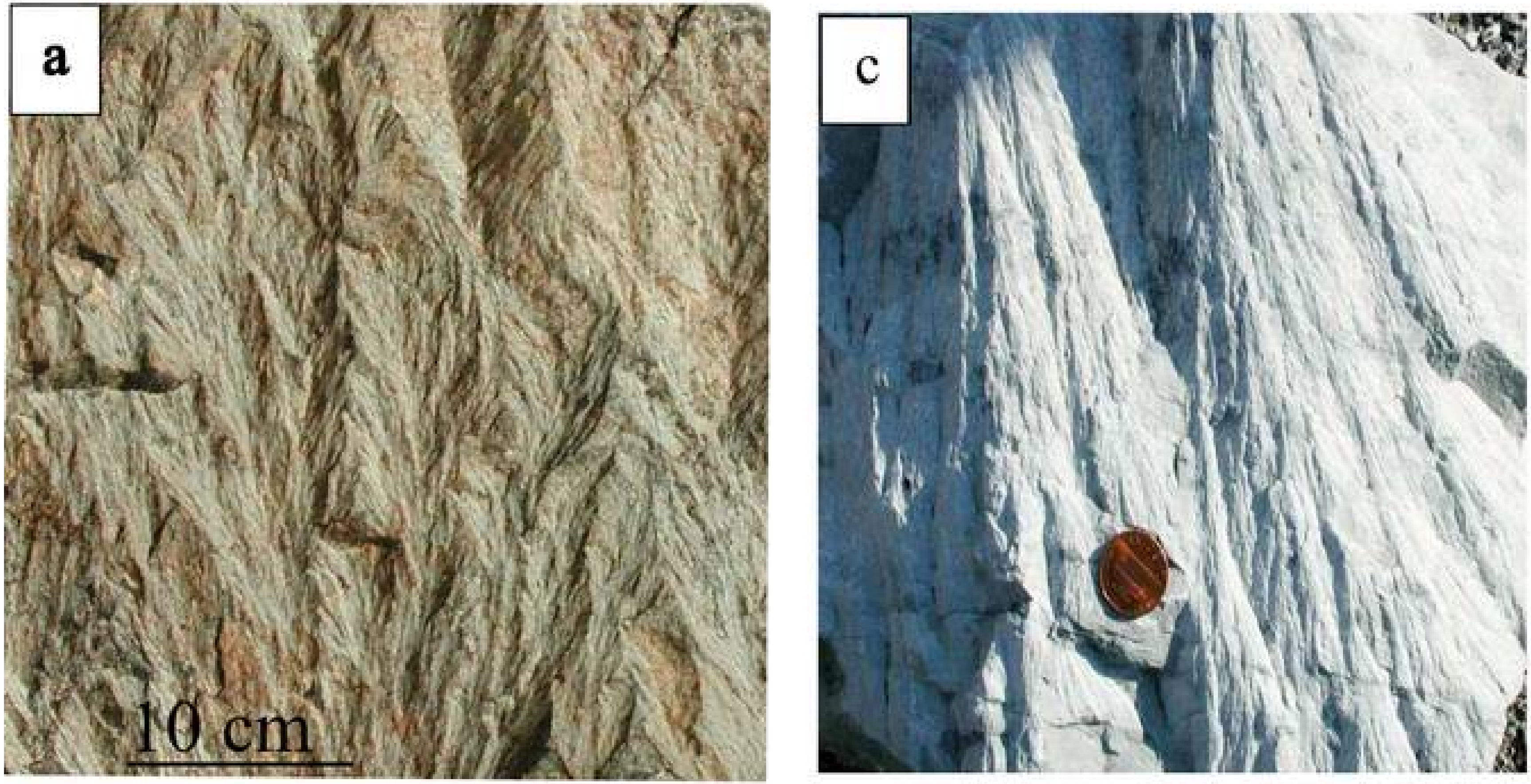

Figure 21: Shatter cones from Vredefort (left) and Kentland quarry, Indiana, USA (right). From Sagy et al., 2004.

4.6 Rupture velocity – shatter cones and plumose structures

The angle of the shatter cone is a function of rupture velocity. This follows from new insights into “crack front waves” which are localized waves that propagate along the leading edge of a propagating crack. They are generated by the interaction of a crack with a localized material inhomogeneity (Sharon et al., 2002). A narrower angle of the cone indicates higher velocity, in the limit reaching that of the Rayleigh wave.

This theory was applied to show how the velocity of rupture forming shatter cones decreased with distance from the Vredefort impact (Figure 22 and Figure 23).

The same theory suggests that the rupture velocity for a particular mining induced fracture (Figure 13) was faster than that for a naturally formed fracture (Figure 17). We see more about fractographic striations in Session II

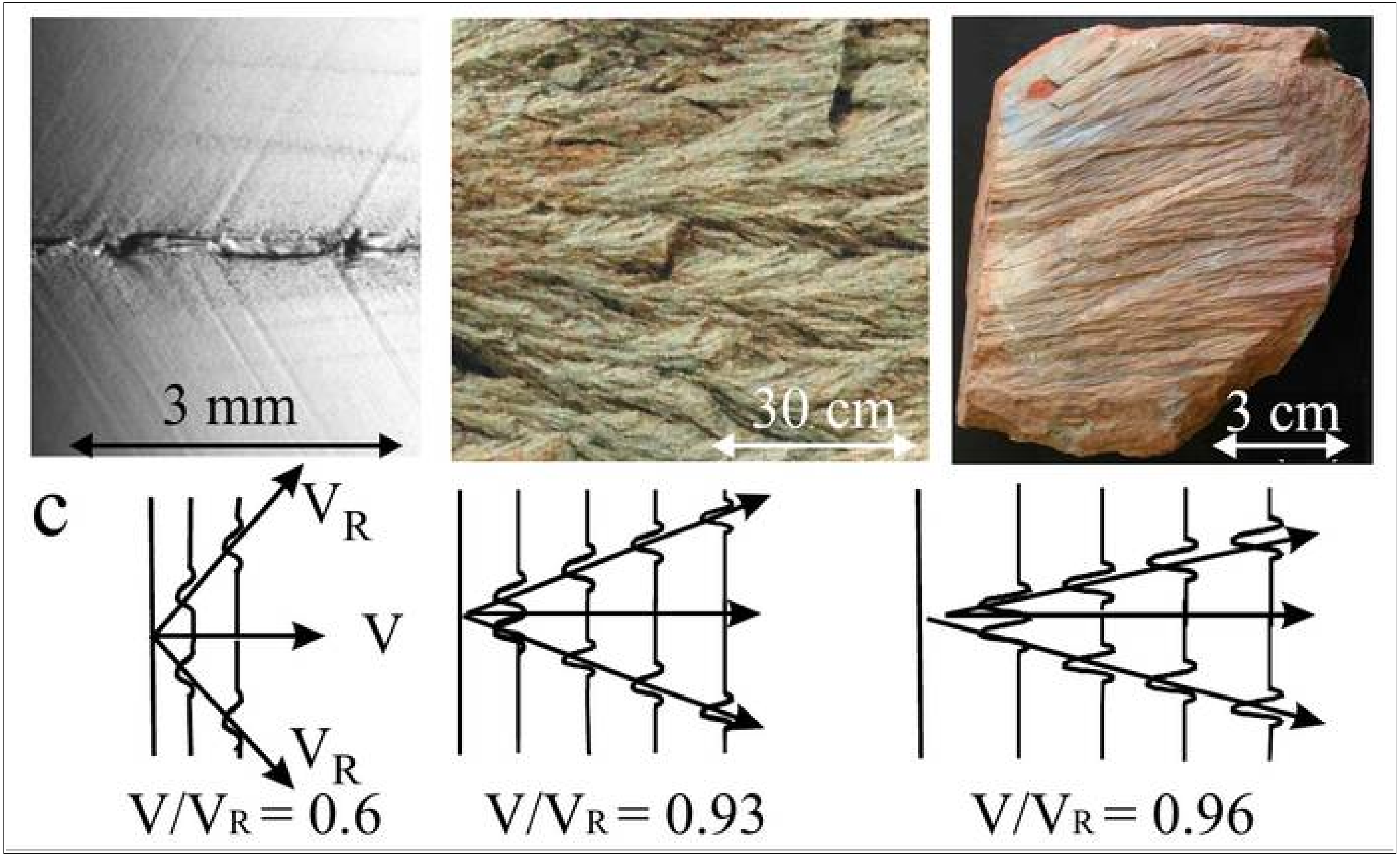

Figure 22: FW marks in glass (left) and V-striations on quartzite (centre) and slate (right) shatter cones with (bottom) accompanying schematic diagrams of FW generation at velocities V/V_R=0.6 (left), V/V_R=0.93 (middle), and V/V_R=0.96 (right), which provide angles a, consistent with the V-angles above. (Sagy et al., 2004).

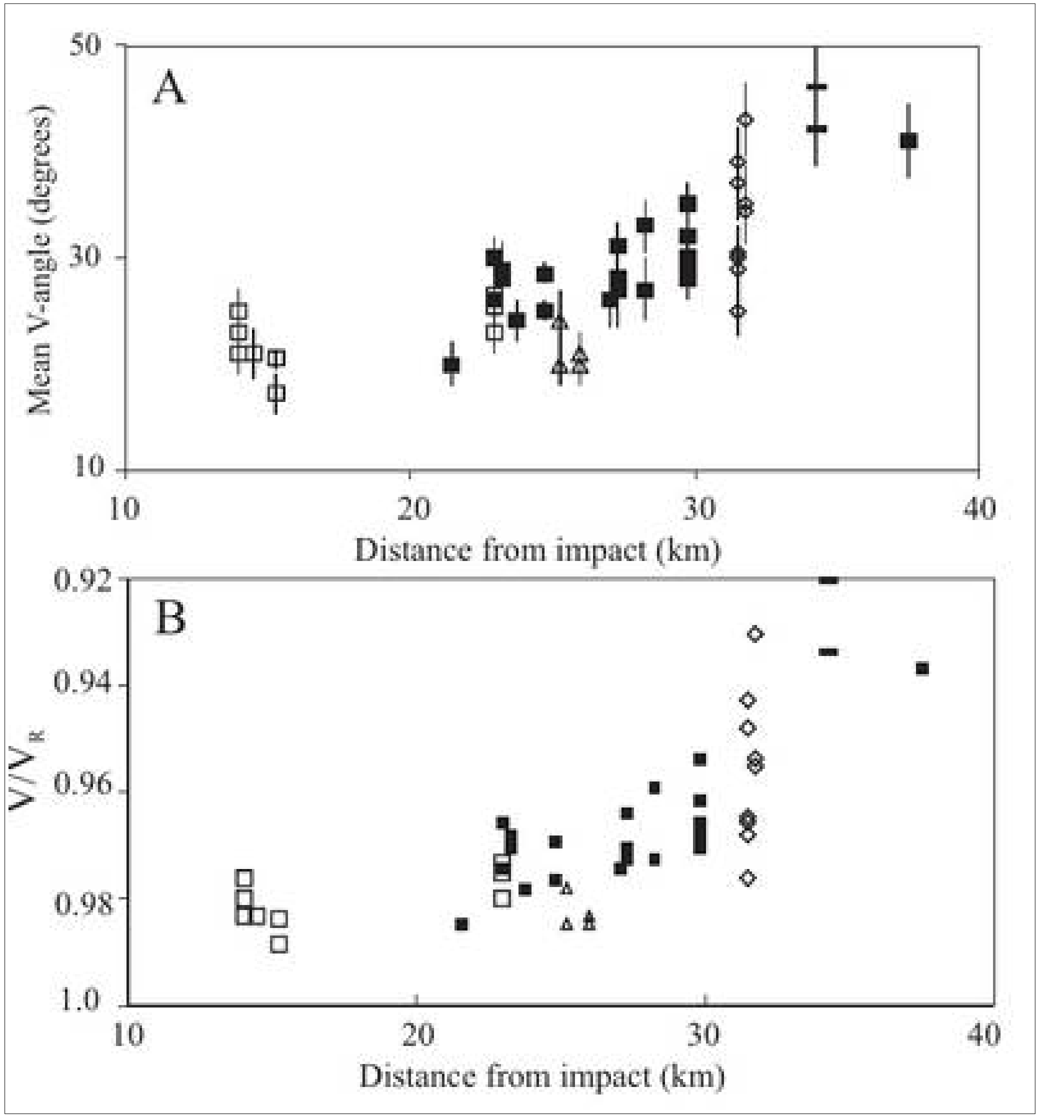

Figure 23: The V-angles of shatter cone striations measured in Vredefort site and the associated propagation velocity,V/V_R (Sagy et al., 2004)..

4.6.1 A word about extension fractures and linear fabrics or striations

We look at slickensides and their meaning in Session II. I shall also point out that the intersection between a set of closely spaced extension fractures and a shear zone wall can yield a prominent set of striations with orientation at right angles to direction of slip or direction of dilation. One must be aware of this since it could be confusing (Figure 24).

Figure 24: A set of closely spaced extension fractures abut against a planar discontinuity (left). If we remove the top plane, we may see a prominent lineation - at right angles to the direction of dilation.

5 Pseudotachylite

We cannot leave shatter cones without considering pseodotachylite (Figure 25). It is beautiful rock with a dramatic history and is found in many places in our gold mines. First described by Shand (1916), the dynamically formed rock type is fairly common along fault zones and also along the VCR as far as the Klerksdorp gold field. Apparently no pseodotachylite has been identified in the Free State gold field. This wide distribution reflects the effects of the Vredefort impact which dynamically affected the whole of the Wits basin. At surface, the radius of the impact crater is estimated at ~300 km (Figure 26)

There is still uncertainty, or rather disagreement, about the age and origin of some occurrences. Cross cutting relations clearly indicate multiple pulses of pseodotachylite, but it is not clear whether it simply results from the complexity of the dynamics during the impact (phases of extreme compression and decompression within seconds) or whether it reflects a protracted geological history. One argument is that, since a set of pseudotachylites are spatially associated with a particular fault and the fault appears to be part of a set of faults that pre-date the deposition of the Black Reef dated at ~2580 Ma (the impact is dated at 2023 ± 4 Ma), we are clearly looking at different geological ages of pseudotachylites (Figure 27). A counter argument is that a small part of the old fault was re-activated and affected by the complex, multiphase dynamics of the impact. I quote Reimold (2012) "..they should consider that major effects of the impact event were tectonic modifications of the entire Witwatersrand basin. Certainly, numerous faults would have been reactivated... oh, and of course, the deformation associated with the impact event would not have been a single-stage event. To the contrary, impact tectonics are complex and multi-stage (initial outward movement of material, shortly followed by the inward collapse of the early transient cavity, and finally outward-directed flow related to the collapse of the central uplift). Each of these stages could have had the potential to generate faults, reactivate faults, and to generate fault rock – indeed, why not multiple generations thereof?"

Is it not fun to be a geologist?

Meanwhile we may simply view in awe the beautiful rocks created by the extreme dynamic strain imparted on selected faults and lithological contact zones (Figure 28, Figure 29).

We may also observe a form of extreme ductile strain. Continued shear deformation along the fault zone filled with viscous molten rock may cause shearing and folding and, ultimately sheath folding. Imagine the active shear zone containing isoclinal folds with fold axes normal to the direction of shear. Since the fold hinges will not be absolutely straight, they can themselves be deformed resulting in the sheath folds. I found some of these at the contact between the Green Bar and the quartzite above the CLR at Tautona (Figure 30 and Figure 31).

Figure 25: Beautiful.

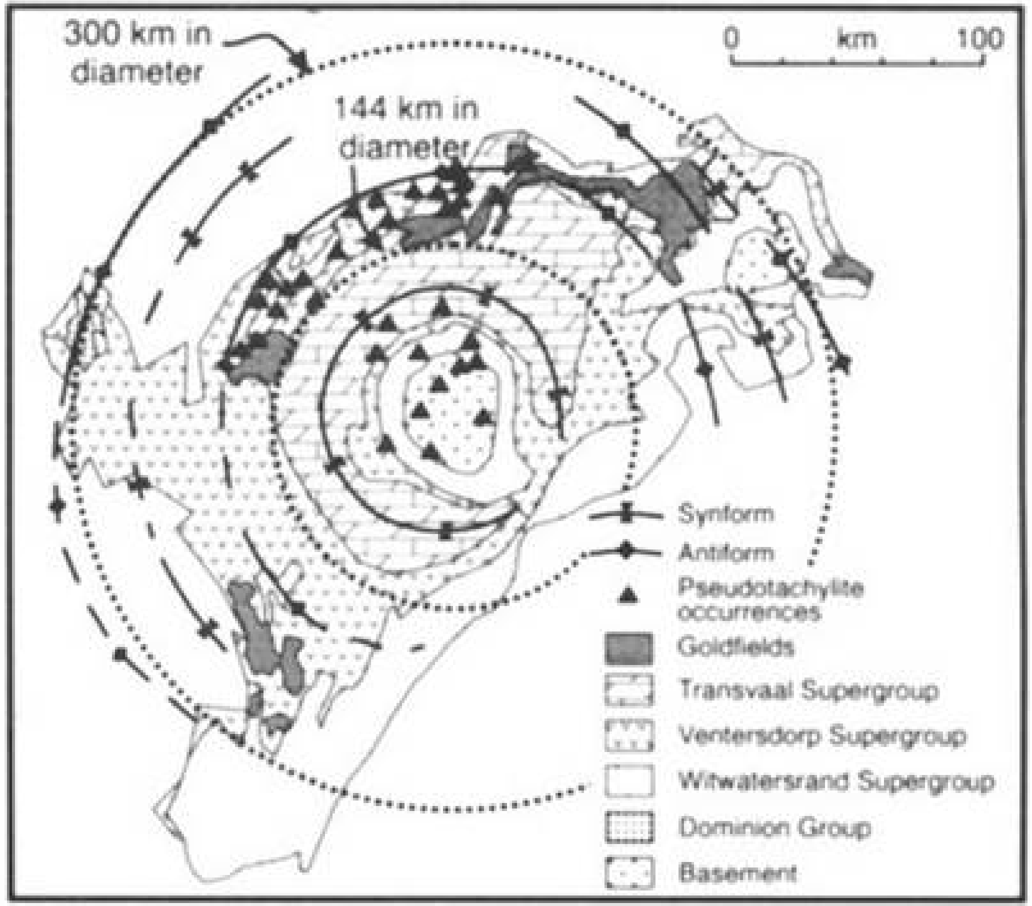

FIG. 4. Distribution of pseudotachylite, large folds and goldfields within the Witwatersrand Basin and in relation to the transient cavity (~144 km) and final rim diameter (~300 km) estimates (dotted lines) of the Vredefort structure. After Fletcher and Reimold (1989) and McCarthy *et al.* (1990).

Figure 26: Figure 4 and its caption from Therriault et al. (1997).

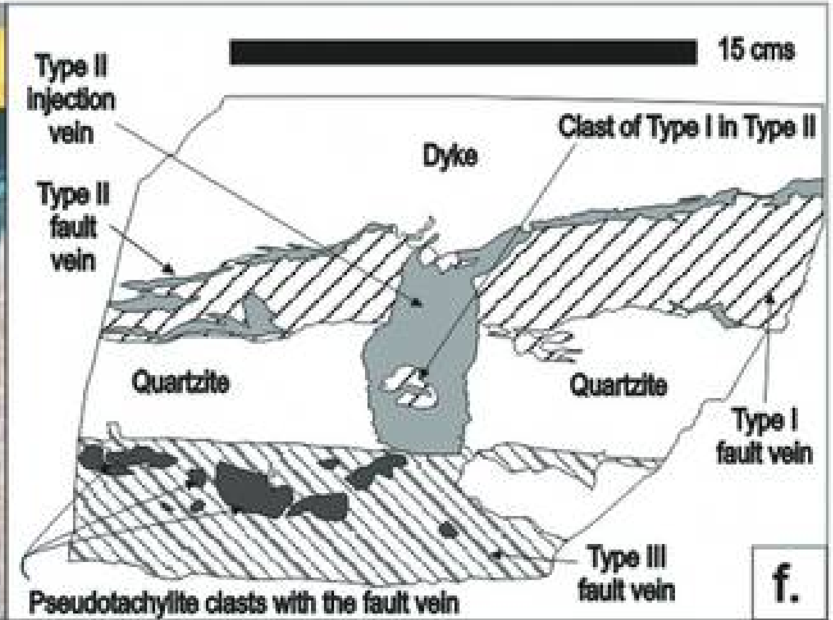

Figure 27: Pseudotachylite in the south boundary fault, Cooke shaft. Apparent multiple phases occur along a fault. Similar faults appear not to breach the base of the Transvaal Basin, dated at ~2580 Ma. The Vredefort impact is dated at 2023 ± 4 Ma.

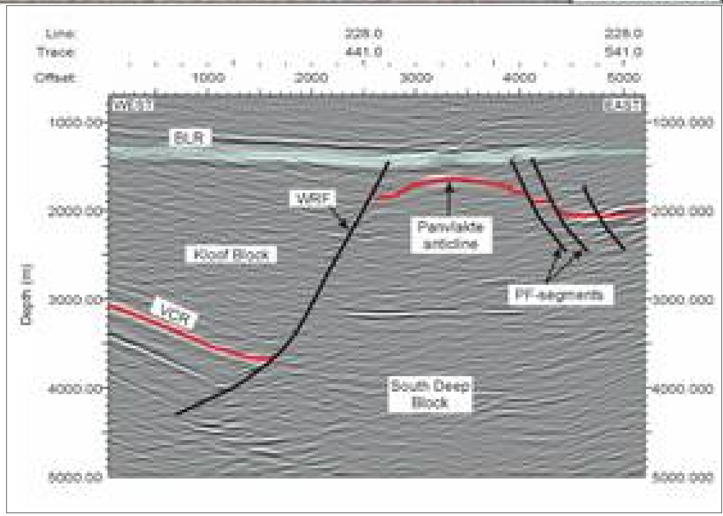

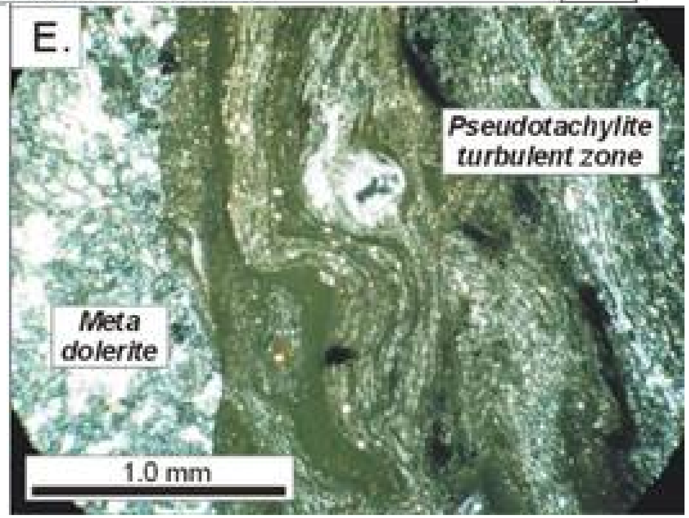

Figure 28: Fault through the VCR at Tau Lekoa

Figure 29: A zoom in on the pseodotachylite.

Figure 30: Pseudotachylite along a bedding plane fault below the Green Bar at TauTona

Figure 31: Same as above, with banding within the pseodotachylite outlined.

6 Nature of deformation controlled by rock characteristics

Books can be written about the differences in response to loading by different rock types and different loading environments. Here we simple look at a few examples of different responses to mining induced stress by differences in rock types. In some cases the differences appear subtle, but the difference in response is significant.

6.1 Brittle vs “ductile”

In deep, hard rock mines, we obviously work in the brittle domain and we generally pay no attention to ductile strain phenomena. I have, however, seen brittle shear failure in the CLR hangingwall, associated with apparently ductile failure in the overlying Green Bar (Figure 32, Figure 33). The loading conditions were high stress (~3000m below surface), high confinement (assuming the deformation took place far ahead of the advancing face) and at possibly at 45˚C or higher. The photograph suggests these conditions were conducive to brittle deformation in the quartzite and ductile deformation in the shale. The “ductile” here refers to the absence of brittle deformation features and probably not true ductile deformation as in the high grade metamorphic rocks or viscous pseudotachylites.

6.2 Shear fractures vs extension fractures.

We are blessed to be able to study extension fractures and shear fractures in our mines with a reasonable understanding of the stress conditions under which they have formed. For example, the stress 2m ahead of a CLR stope at Tautona would be high and would not be expected to differ in the vertical sense over a few cm. So the differences in the frequency of extension fractures vs shear fractures as shown in Figure 34 and Figure 35, must be attributed to difference in shear moduli, the slightly more argillaceous quartzite yielding in shear and the cleaner quartzite bed above it yielding in extension. A similar phenomenon was observed at Hartebeestfontein mine – Koos Bosman shared photographs form a rockburst site in 2008 (Figure 36).

Figure 32: Photograph of the contact between the Green Bar (shale) and the quartzite above the Carbon Leader Reef, Western Deep Levels, many years ago.

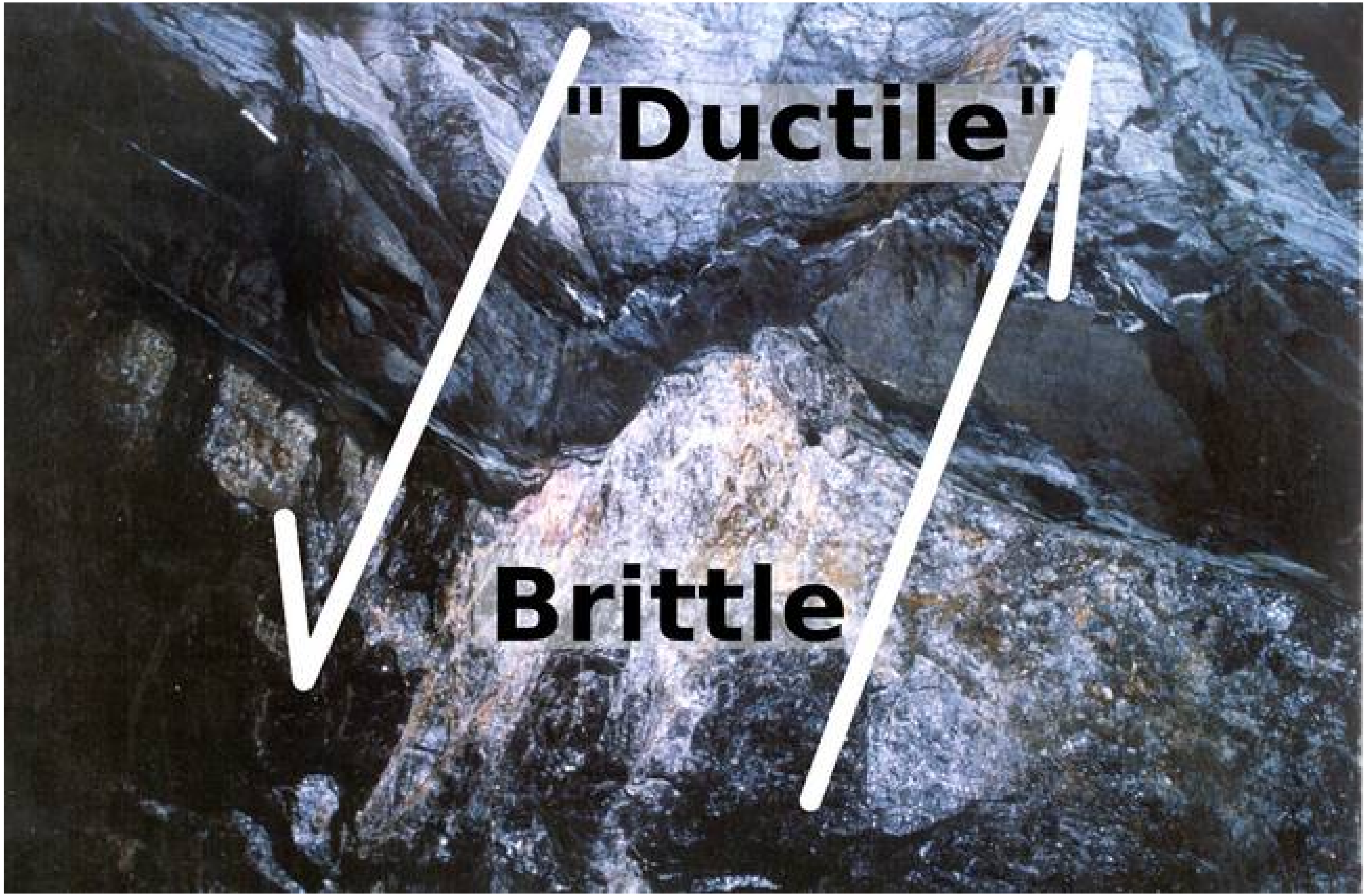

Figure 33: Same as above, with annotation.

Figure 34: Fractures in the sidewall of a CLR stope at TauTona

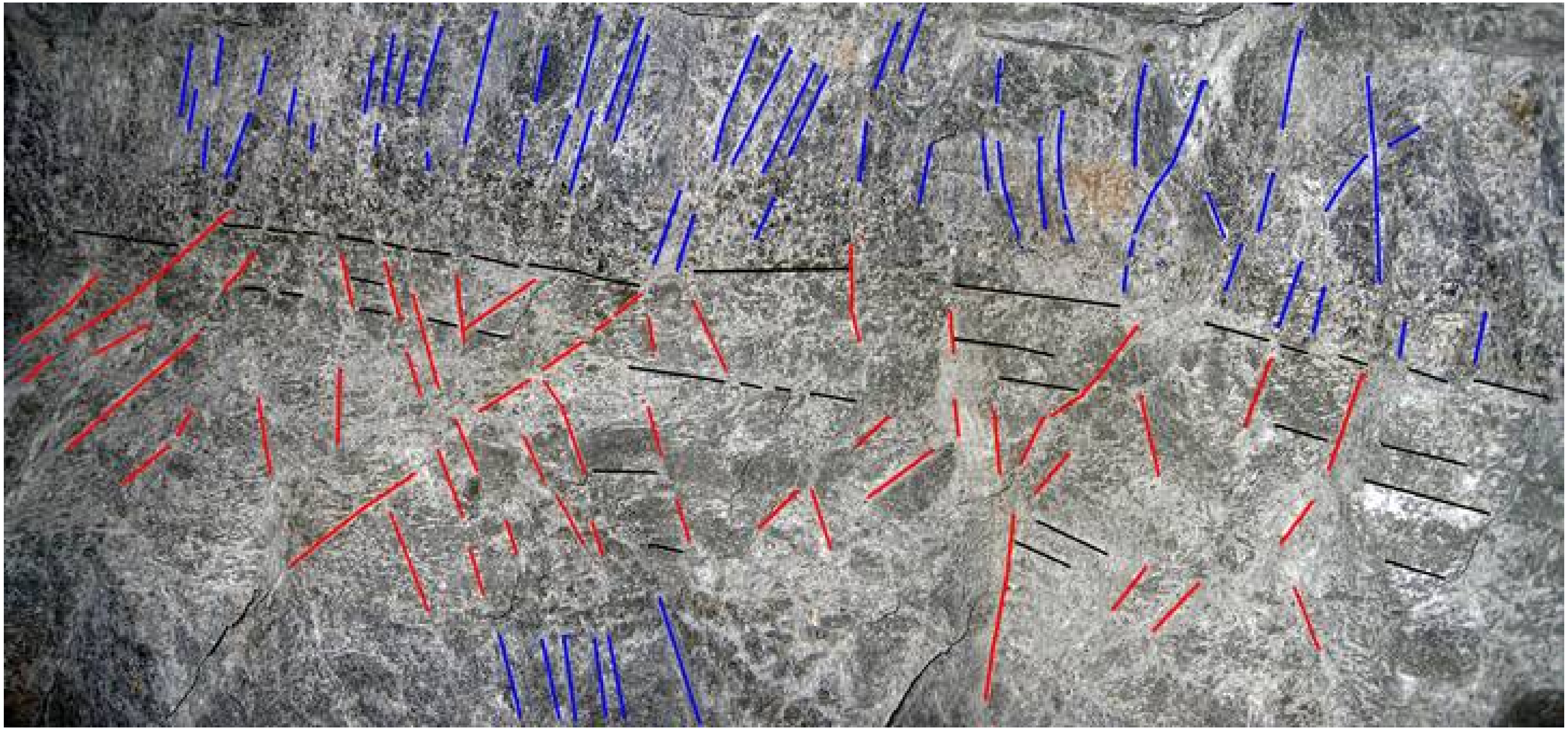

Figure 35: Same as above, with annotation. Blue lines depict extension fractures while red lines depict shear fractures. Black lines is bedding.

Figure 36: Similar to the above, from the Hartebeestfontein mine (thanks Koos Bosman).

6.3 Ortlepp shears in different rock types

Ortlepp shears are considered in some detail in Session II, but here I simply want to show how the shear mechanism manifests in different rock types.

During a rockburst site visit at Mponeng in the mid nineties, we saw an Ortlepp shear daylighting at the face (Figure 37, on the right). Whether this particular shear was associated with the particular rockburst is unclear. It was noticed that the same dynamic brittle shear through the VCR had quite a different signature in the lava hangingwall.

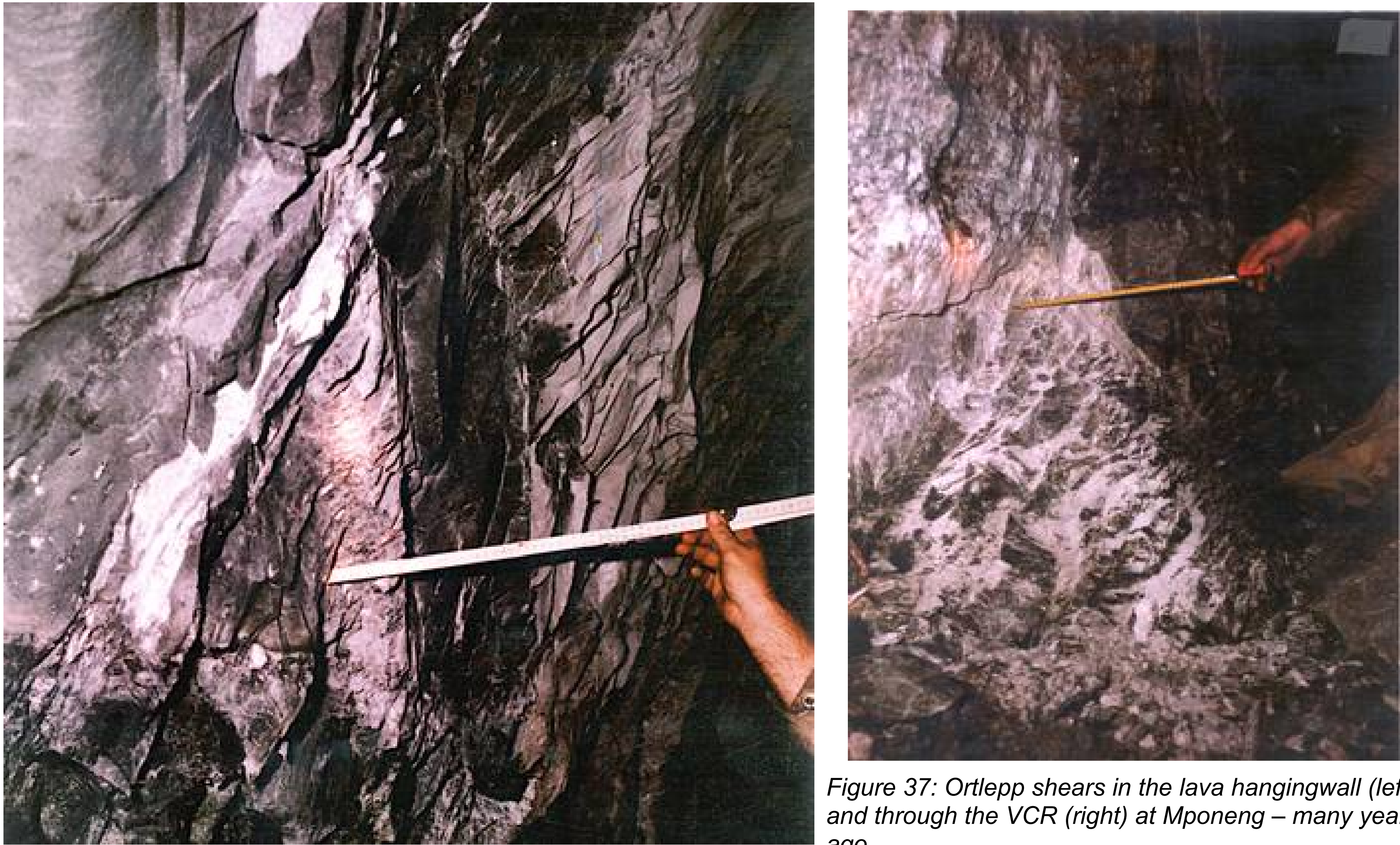

Figure 37: Ortlepp shears in the lava hangingwall (left) and through the VCR (right) at Mponeng – many years ago.

7 Shear zones

Shear zones have, of course, been discussed above and more will come in Session II, but here I need to point out particular aspects.

7.1 Ductile shear zones

We briefly considered ductile vs brittle shear zones above. We look at a few more examples here of ductile shears here (Figure 38). Ductile shear zones are characterized by penetrative shear fabrics reflecting the orientation of strain, maximum strain at the centre and less so towards the shear zone walls (Figure 38). Extreme ductile strain yield sheath folds as we saw above.

Figure 38: Classic ductile shear in granite (left) and in meta-sediments (top right) NOT to be confused with cross-bedding (bottom right).

7.2 Brittle shear zones

7.2.1 General description of mine fractures

The second most abundant mining induced structure after extension fractures are shear fractures. These are brittle shear zones, often of dynamic origin (Ortlepp shears). One of the best known figures describing fractures around gold mine stopes is that of Adams et al., (1981) - (Figure 39). We updated the nomenclature in 2012.

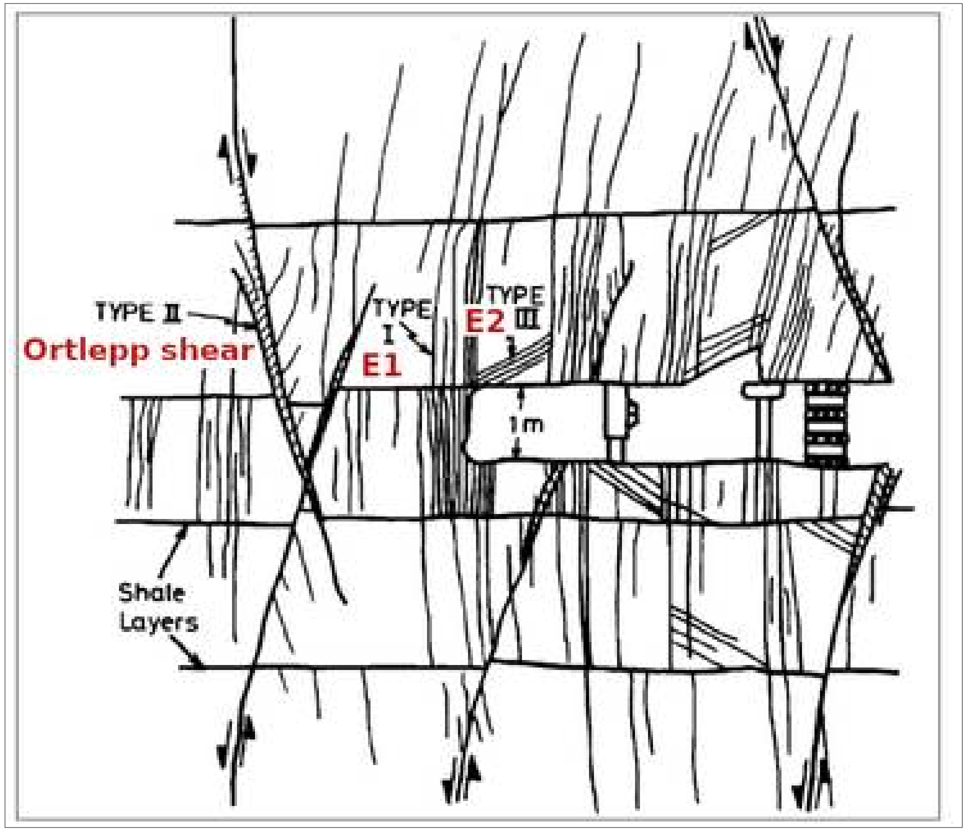

Figure 39: Reproduction of Figure 2 of Adams et al. (1981) showing the distribution of fractures around a stope face. Their "Type II" we refer to as Ortlepp shears, "Type I" as E1 extension fractures and "Type III" as E2-extension fractures (van Aswegen and Stander, 2012).

7.2.2 Transpressional vs transtensional shear.

The concept is shown in Figure 40 and Figure 41 and explained in detail in van Aswegen and Stander (2012) and discussed again in Session II. Since our 2012 interpretation of the origin of the low-angle fractures (E2-extension fractures, Figure 39), it was interesting to note natural occurrences of high-angle extension fractures in transpressional tectonic environments (Figure 42, Figure 43 and Figure 44).

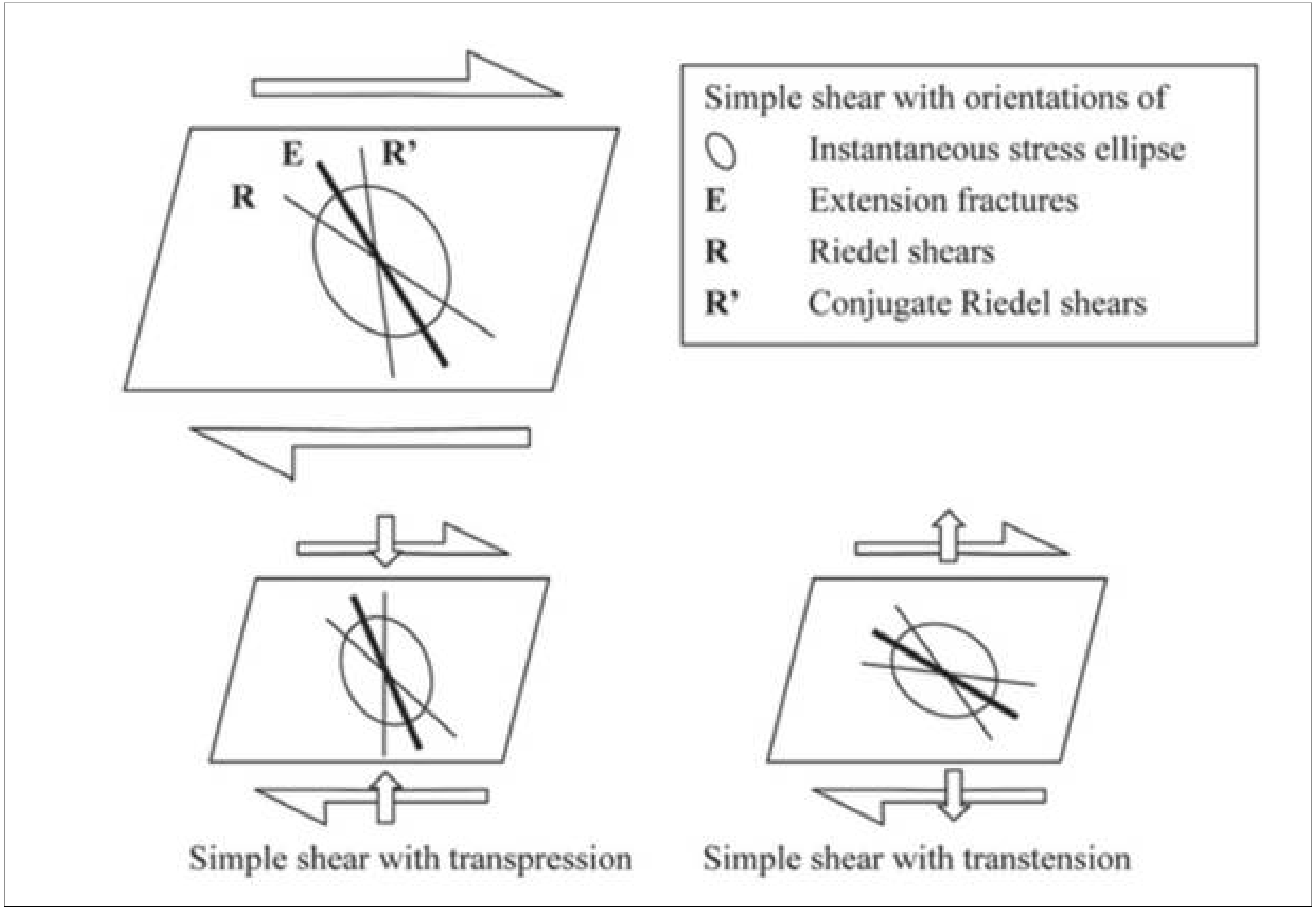

Figure 40: Geometric relationships between shear zones, extension fractures and Riedel shears. Note that the extension fractures form under conditions of infinitesimal strain and the schematic depiction of strain is here exaggerated

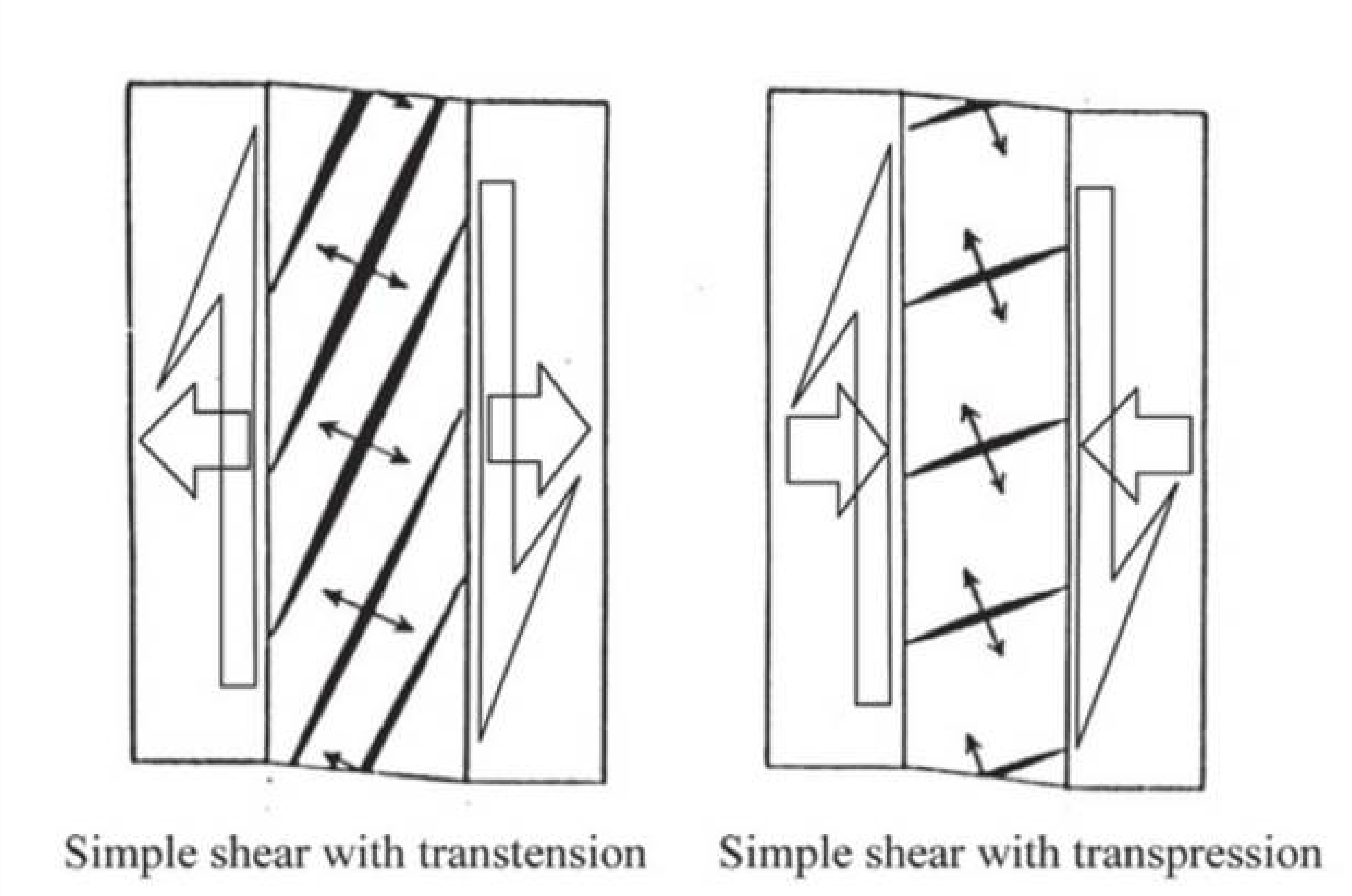

Figure 41: Orientations of shear zone vein arrays – redrawn after Ramsay and Huber, 1983, Figure 3.21

Figure 42: Extension fractures in a sandstone bed amongst sheared shale - Peninsular Formation, TMS, Stanford's Cove, Gansbaai

Figure 43: Extension fractures in a sandstone bed amongst sheared shale - Penisular Formation, TMS, Stanfords Cove.

Figure 44: One possible interpretation of the origin of the extension fractures above. The red arrows depict tectonic load and the grey arrows depict material flow during folding.

7.2.3 Curved extension fractures

In the natural environment we may see extension fractures deformed by later tectonic deformation (Figure 45).

In mines, however, we are used to extension fractures curving around tunnels (bow wave structure) and stope faces, as they trace the $\sigma_1\sigma_2$ surface – <u>at the time of fracturing</u>.

It was interesting to see curved extension fractures in the natural environment – always linked to shear deformation (Figure 47). In the case of Figure 47 the curving extension fractures are explained as follows: The overall fracturing results form trans-tensional shear and the fractures are parallel to the $\sigma_1\sigma_2$ surface. Rigid blocks, however, resist fracturing and transpressional load develops within the block. This change from transtensional to transpressional strain within the rigid block is gradational resulting in the curvature of the resultant extension fracture.

Figure 45: A very poor copy of a figure from Ramsey and Huber (1983) showing early extension fractures within a shear zone, filled with vein quartz, deformed by further shearing later on.

Figure 46: Curving extension fractures - we see it all the time ...

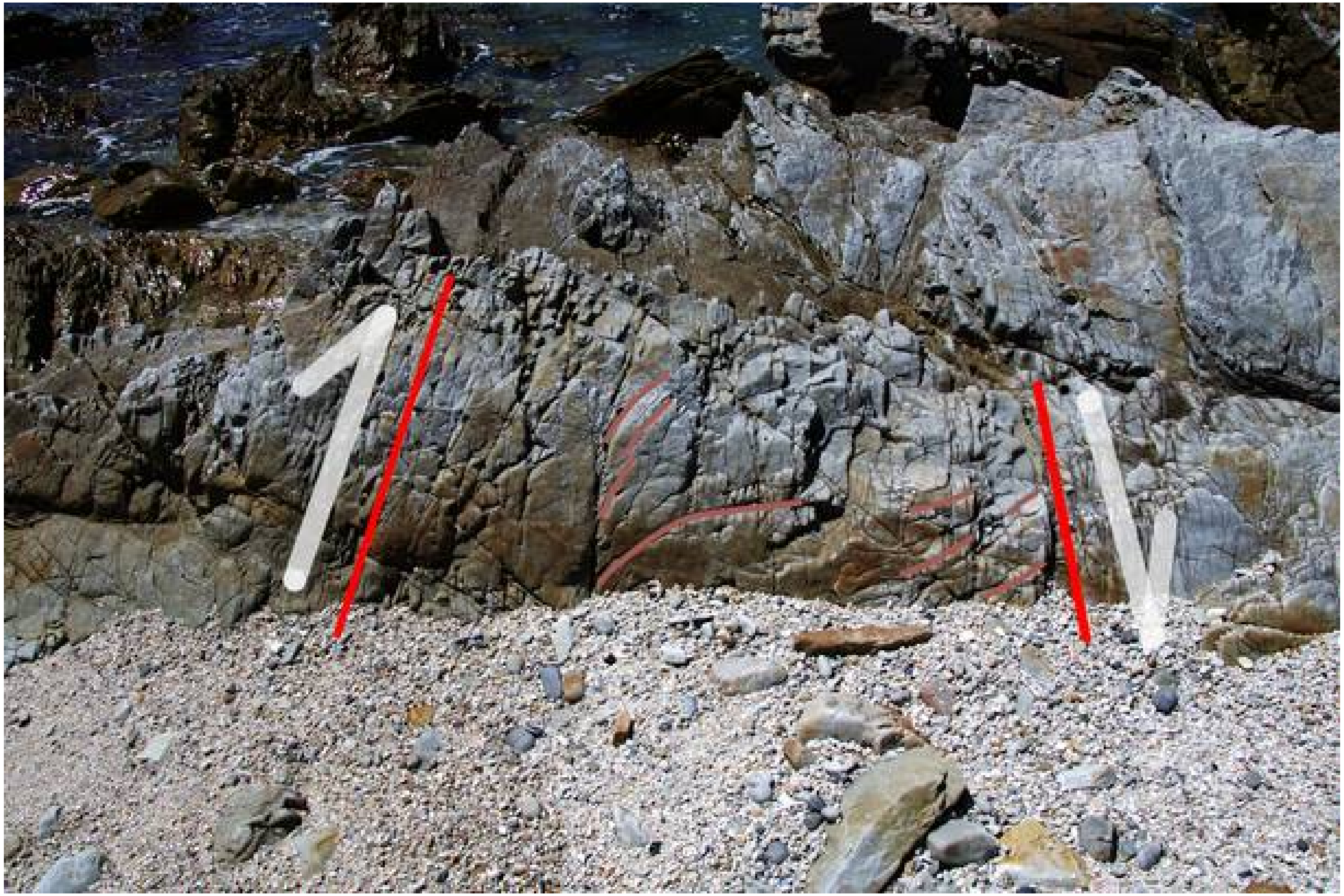

Figure 47: Curving extension fractures in a brittle shear zone near Kleinbaai

8 Notes on stress anomalies

We are confronted with apparently unexplained stress patterns or ‘pockets’. With the above background, we may speculate that a lot of stress anomalies result form stress deflection through elastic shear strain caused by primary variation in rock strength and the nature of the rock fabric. Combining the ideas of stress re-orientation through elastic shear strain and then considering the concept of scale invariance leads to interesting ideas.

8.1 Stress orientation in the West Rand

Considering only gravitational loading as a vertical force on the thick package of south-south-east dipping strata consisting mostly of brittle quartzites separated by weaker shales, the rotation of stress through a mega-shear zone, being this sedimentary package, may explain the major principle stress steeply plunging steeply towards the NNW. More than 20 years ago we actually showed that the concept is not too stupid (Map3D modelling by Ronald Lachenicht).

Something similar is shown in Figure 48. This also leads to the next section.

8.2 Stress channelling

Stress distribution in mega fault zones have been shown to be controlled by differential yielding. An example is given by Baird et al (2009) – see Figure 49 to Figure 51

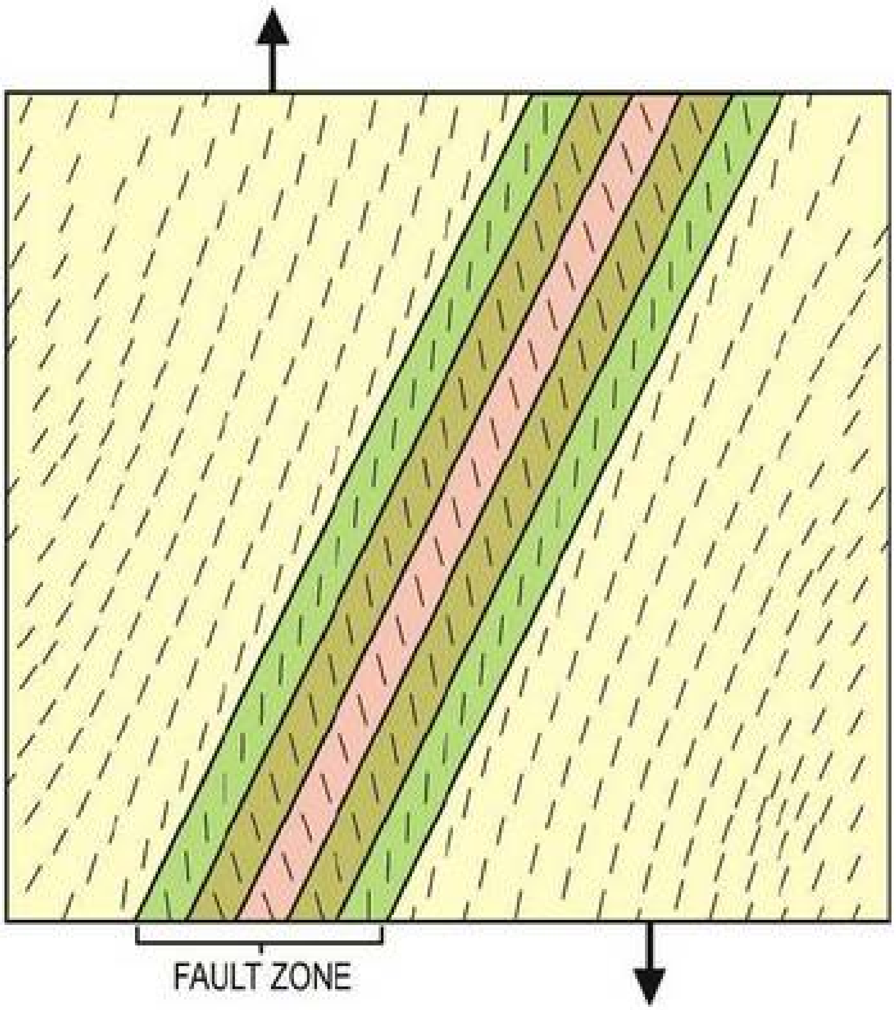

Figure 48: Fig. 11. of Gudmundsson et al. (2010). Finite-element model of the stress trajectories of σ3 in a fault zone composed of a core with a Young's modulus of 1 GPa, an inner damage zone with a Young's modulus of 5 GPa, and an outer damage zone of Young's modulus of 10 GPa located in a host rock with a Young's modulus of 40 GPa. The fault zone is subject to oblique loading, a tensile stress of 5 MPa. The trends of σ3 differ between the core and the damage zone and the damage zone and the host rock, as well as between the sub-zones of the damage zone. This model demonstrates the variation in the local stresses within a typical "layered" fault zone.

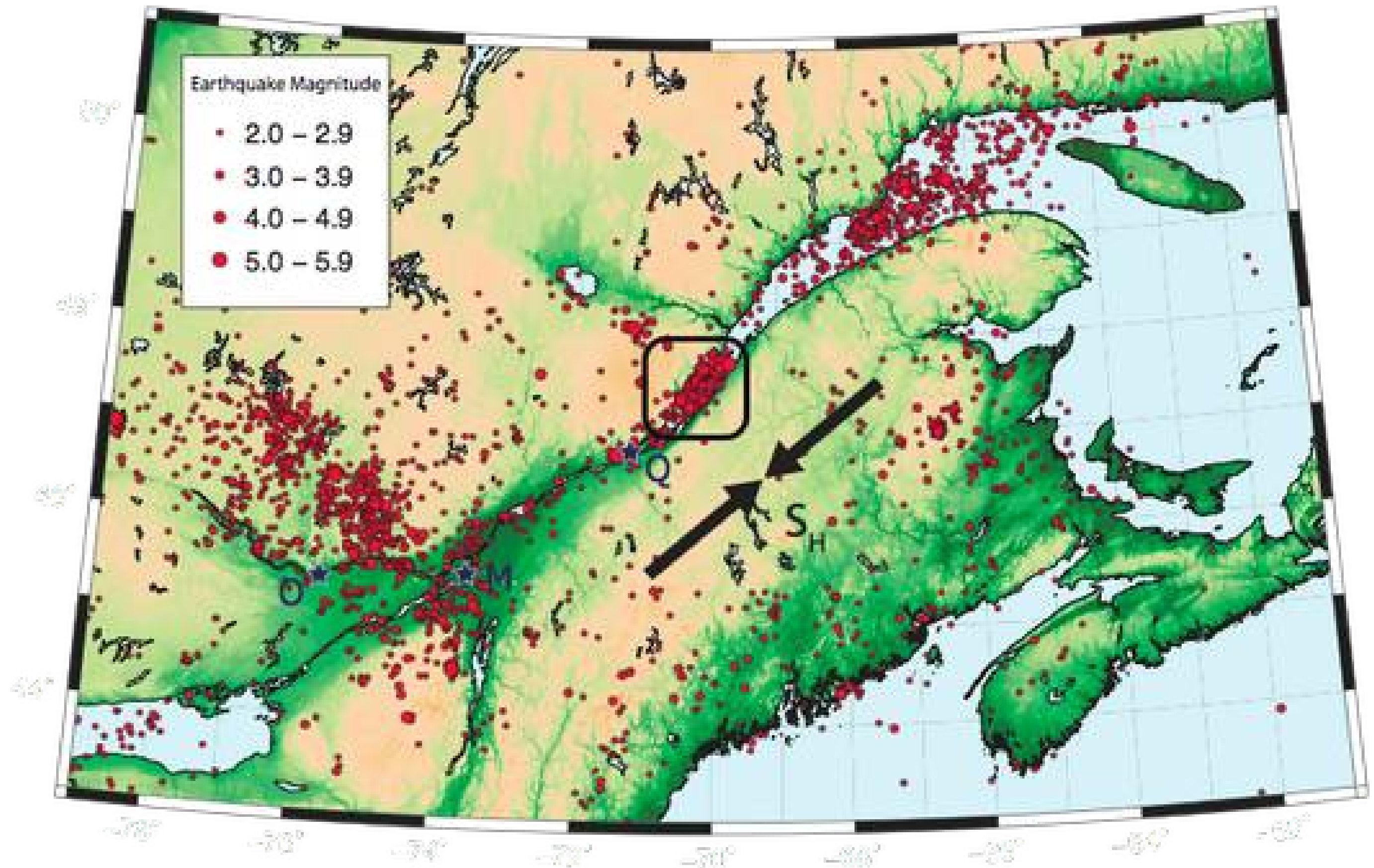

Figure 49: Seismicity map of eastern Canada, showing the location of the Charlevoix seismic zone. Inverted arrows show the dominant orientation of maximum compressive stress (S H)

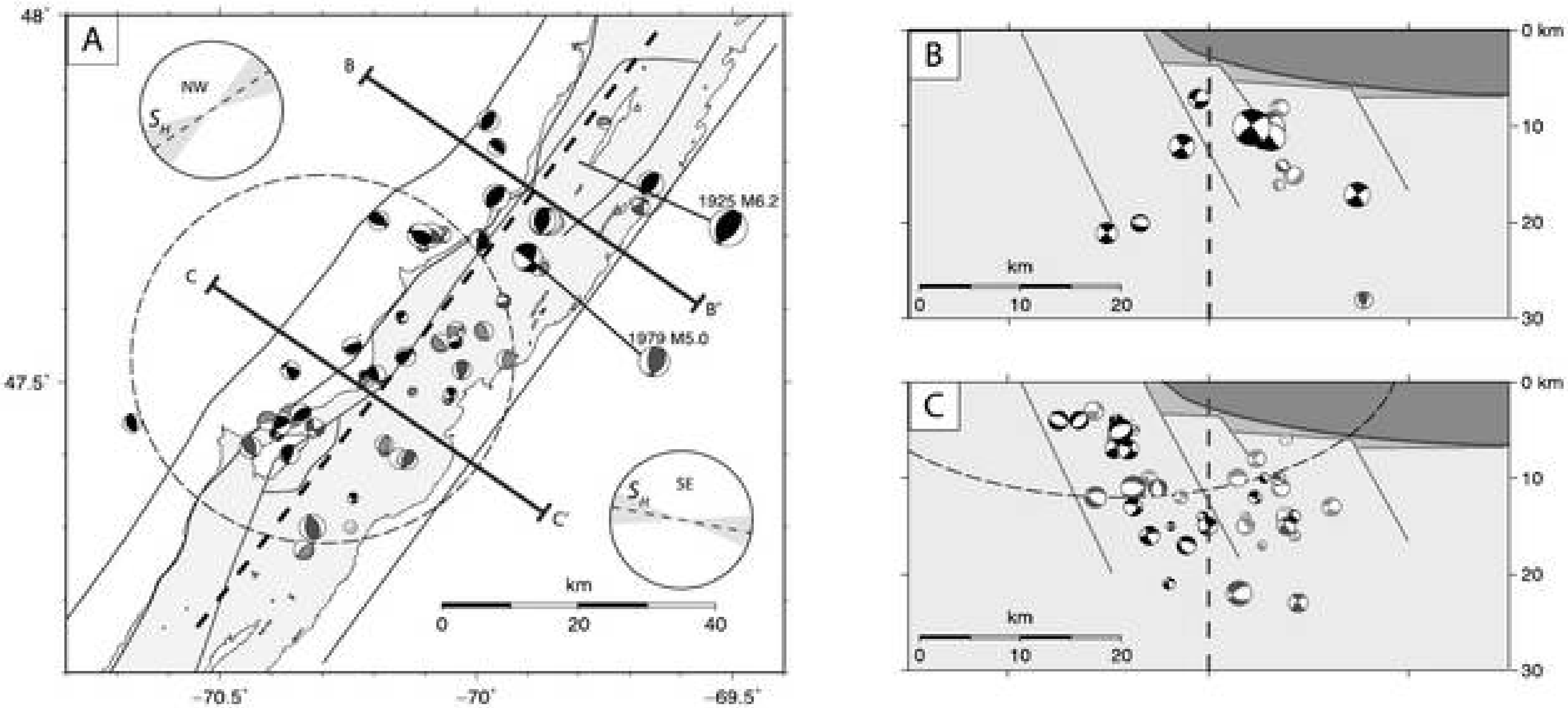

Figure 4. (a) Earthquake focal mechanisms from the Charlevoix seismic zone. Mechanisms are scaled by magnitude. Black, dark grey, and light grey mechanisms refer to quality rankings of A, B, and C, respectively. The two largest events (*M* 6.2 1925 event and m_N 5.0 1979 event) are indicated. Circles with dashed lines and grey angular sectors indicate the average and 90% confidence regions of the maximum horizontal compressive stress direction in the NW and SE clusters of seismicity from the stress inversion of *Mazzotti and Townend* [2010]. (b) Cross section showing mechanisms northeast of the crater. (c) Cross section showing mechanisms within or below the crater. Thick dashed line indicates the separation of the NW and SE clusters of seismicity used in the analysis.

Figure 50: Figure 4 and its caption from Baird et al., 2009.

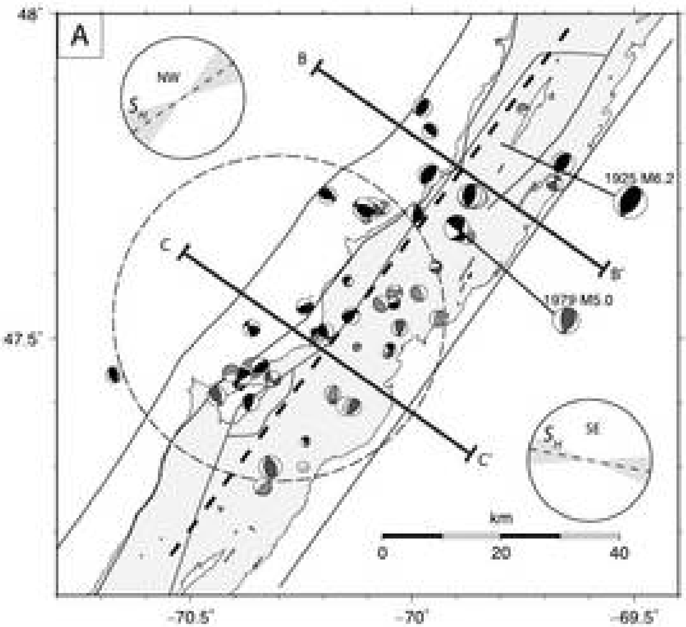

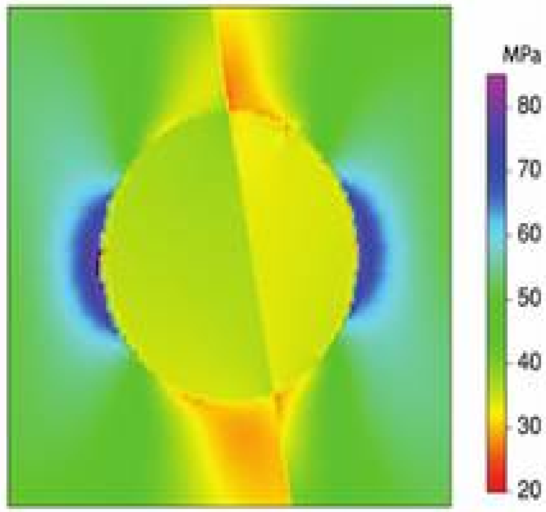

Figure 7. Contour plot of deviatoric stress showing the effect of only a single weak rift fault. The impact structure modulus is set to 50 per cent of the background level and fault friction at 5°. In this case, since there is no region bounded on both sides by faults, stress simply flows around either side of the crater.

Figure 51: Figure 7 and its caption from Baird et al., 2009.

8.3 The Bushveld stress

Underground observations may be confusing (Figure 52, Figure 53 and Figure 54), but recent work does explain the origin of the stress orientation in the Bushveld as being the result of flexural slip (i.e. induced shear strain as layers move relative to each other during the down-warping of the strata) as the basin appears to still “sink” (Figure 54). More recent work indicates neo-tectonic activity consistent with the flexural slip theory at < 175000 years (Figure 56 and Figure 57).

The problem is with the continued “sinking” of the basin – how can that be after more than 2000 million years?

I suggested that it is rather because of the ongoing post-Gondwana epeirogenesis, with the granitic KaapVaal Craton rising faster than the more dense Bushveld Complex.

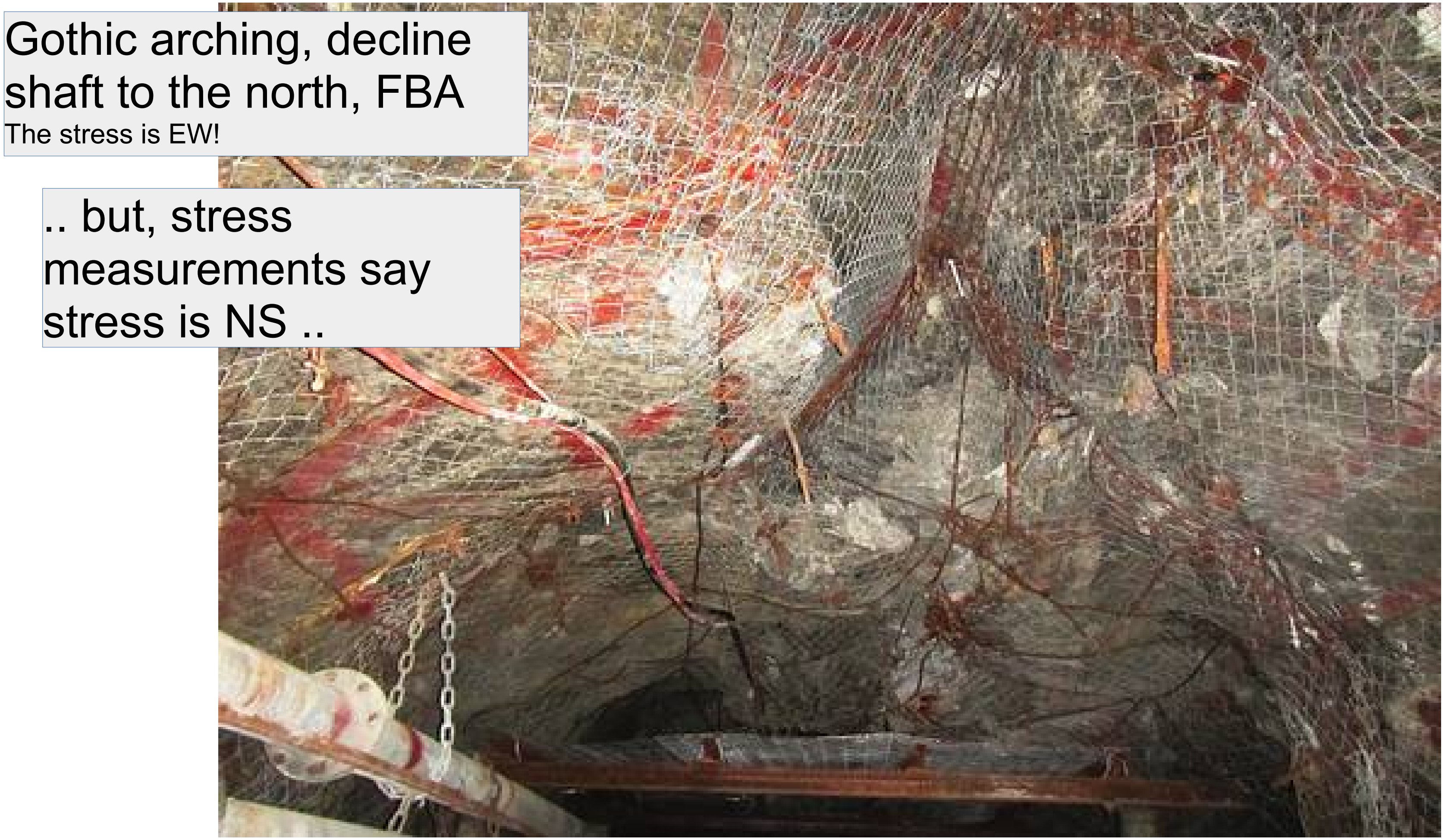

Figure 52: Gothic arching along the decline shaft at the old FBA suggests the major principle strwss is EW

Figure 53: Rockburst mechanism at Siphu indicates principle stress is NS

Figure 54: Rockburst mechanism at Siphu indicates principle stress is NS - again

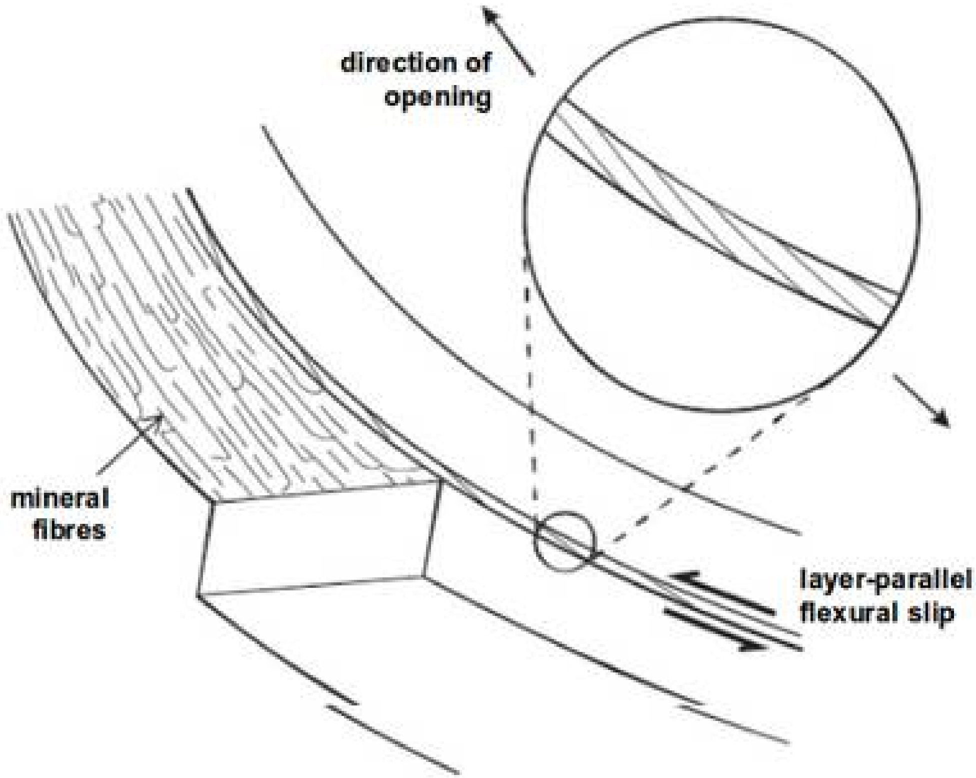

Figure 55: Figure 7 and its caption from Perritt and Roberts (2007)

Fig. 7. Photograph and schematic interpretation (after Price and Cosgrove, 1990) of slickenside "steps" on the hangingwall surface of a layer-parallel fault with reverse dip-slip located along the top contact of the LG6 chromitite exposed at Horizon Chrome Mine, locality A. These slickenside "steps" are a typical feature of the layer-parallel fault surfaces.

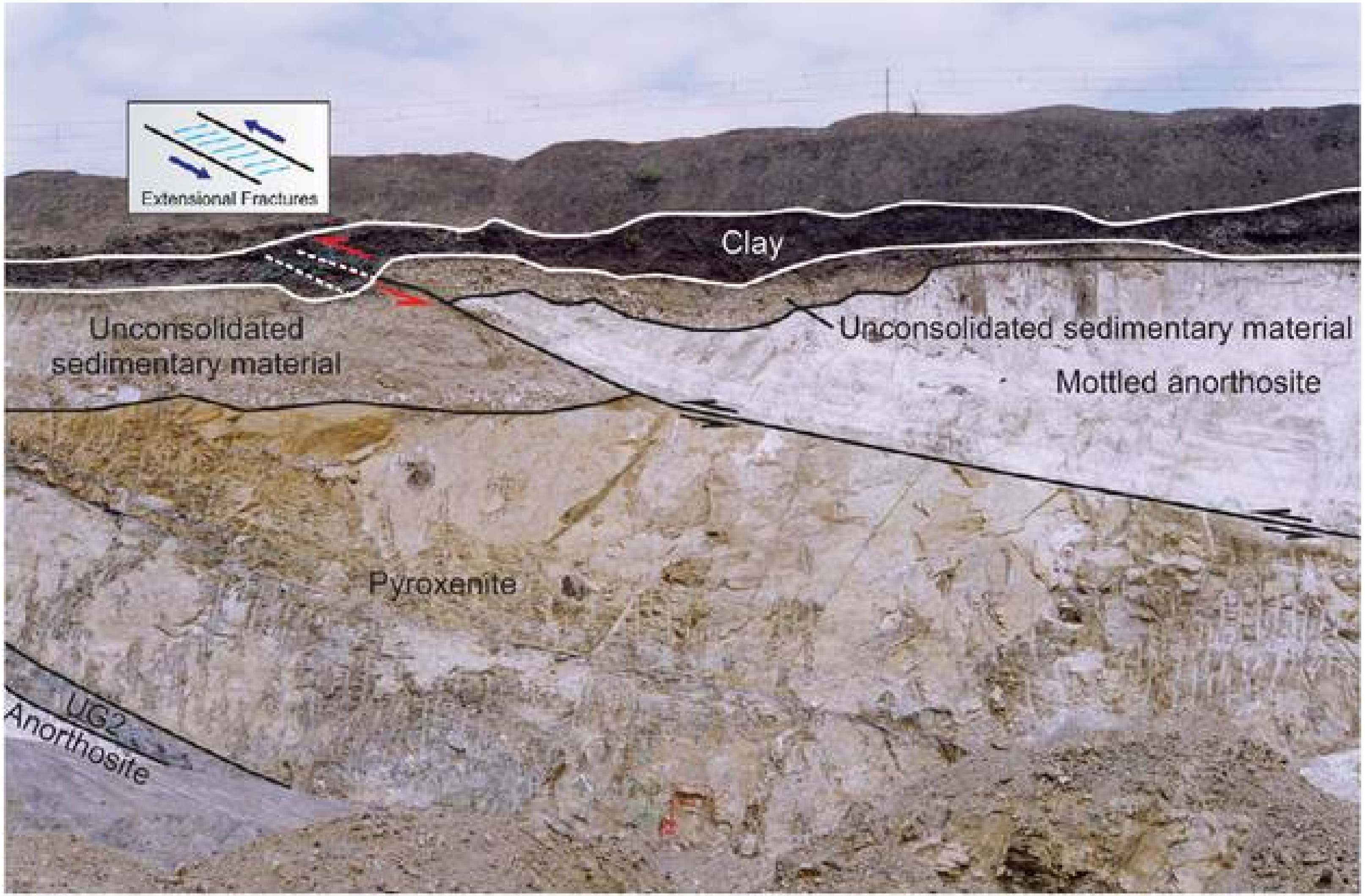

Figure 56: Figure 2. of Steenekamp et al.(2018). Thrust fault in the Sonop area. Note the evidence of a fabric in the clay layer. In the lower left hand corner the UG-2 chromitite layer can be observed. Thickness of UG2 is approximately 1 m and movement of the thrust is approximately 4.2 m.

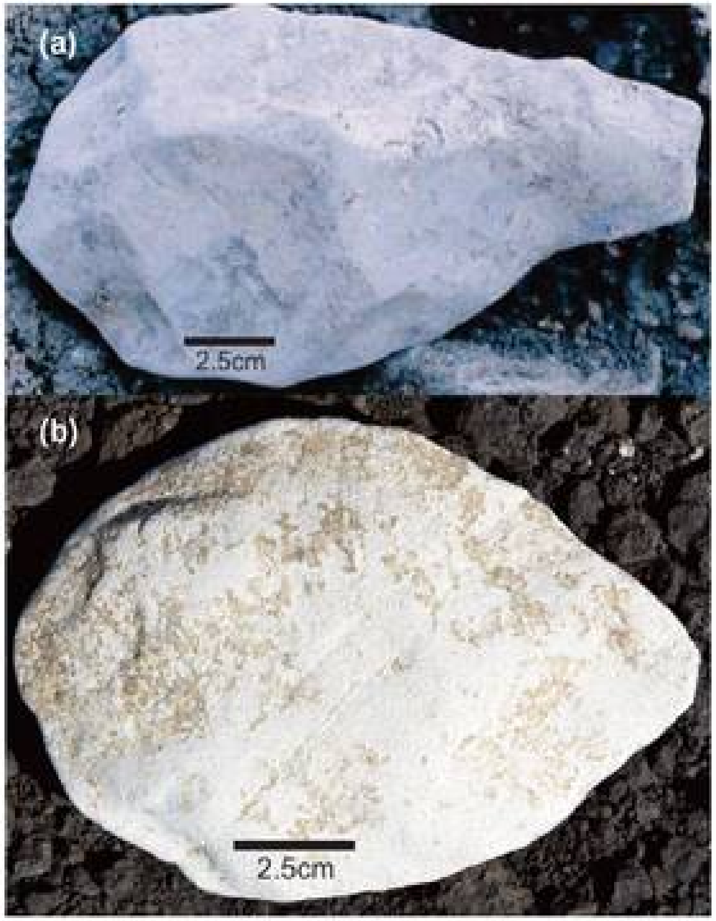

Figure 57: Figure 4 from Steenekamp et al(2018) (a) Acheulian hand axe (Tool 1) found in the unconsolidated sedimentary layer. A second hand axe (Tool 2) was later discovered on the same horizon during mining operations (Table 1). (b) Acheulian hand axe (Tool 2) found in the unconsolidated sedimentary layer underneath the regional clay layer. Note calcrete coating covering the hand axe.

8.4 Stress orientation at El Teniente.

In a similar way we may explain the anomalous stress at El Teniente mine

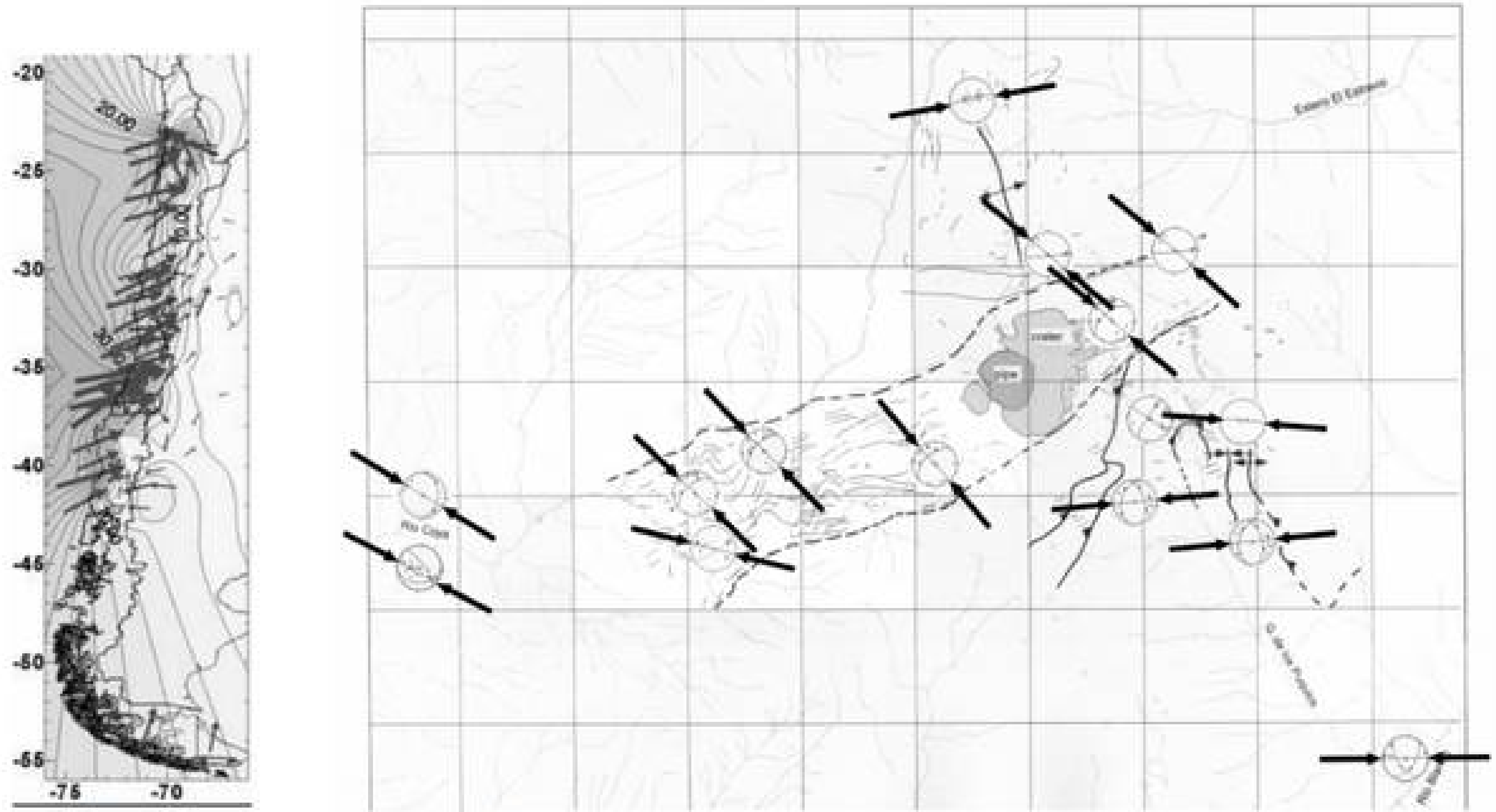

Surface velocity vectors (scaled) on velocity contours (mm/year) for continental Chile.

Windsor, C.R., Caviares P., Villaescusa, E. and Pereira, J. 2006. Reconciliation of Strain, Structure and Stress in the El Teniente Mine Region, Chile. Proceedings of International Symposium on In Situ Rock Stress, Trondheim, Norway.

Figure 58: The stress orientation at El Teniente mine in the Andes tectonic zone is anomalous.

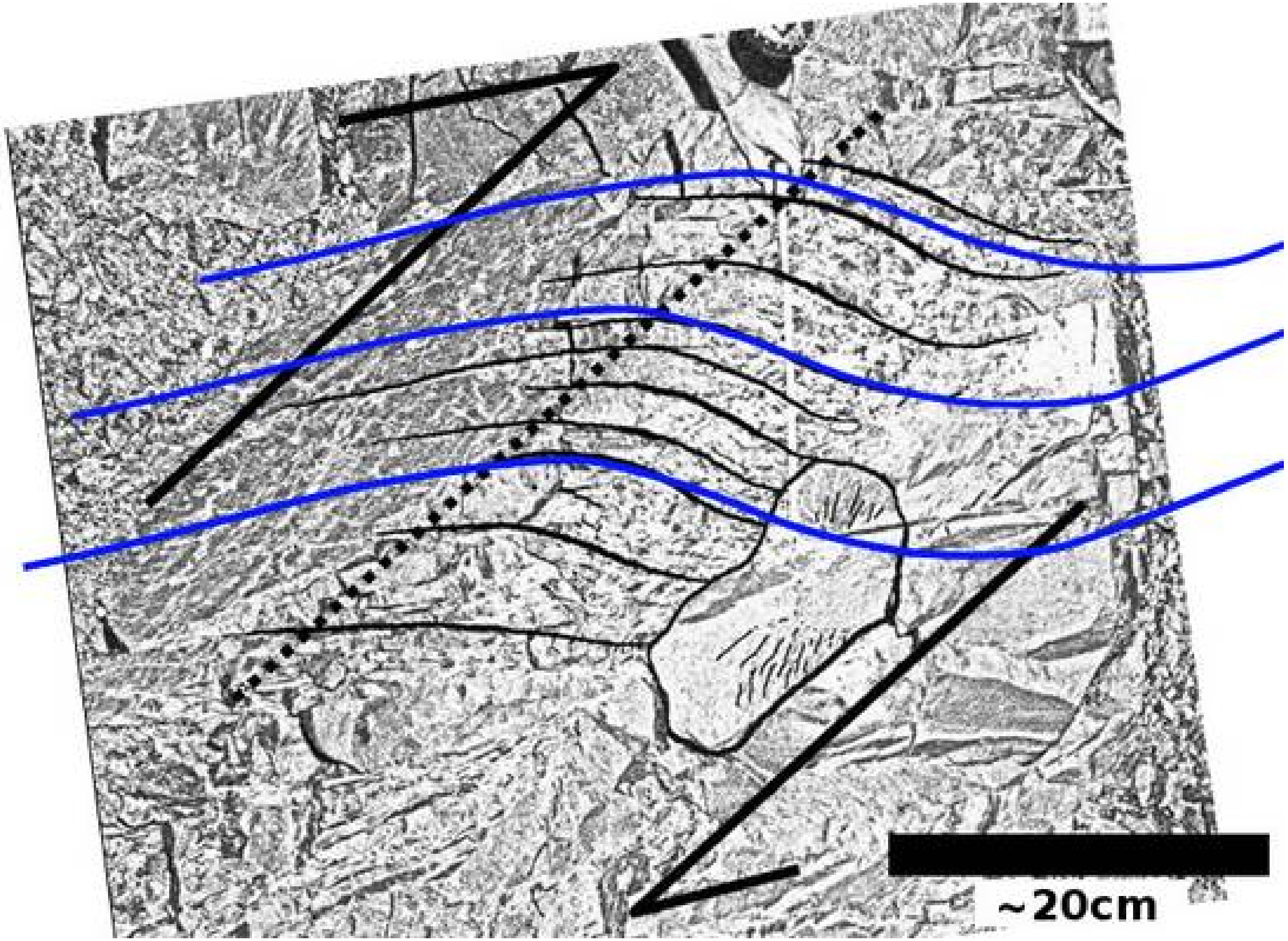

Figure 59: Stress rotation through a brittle shear zone

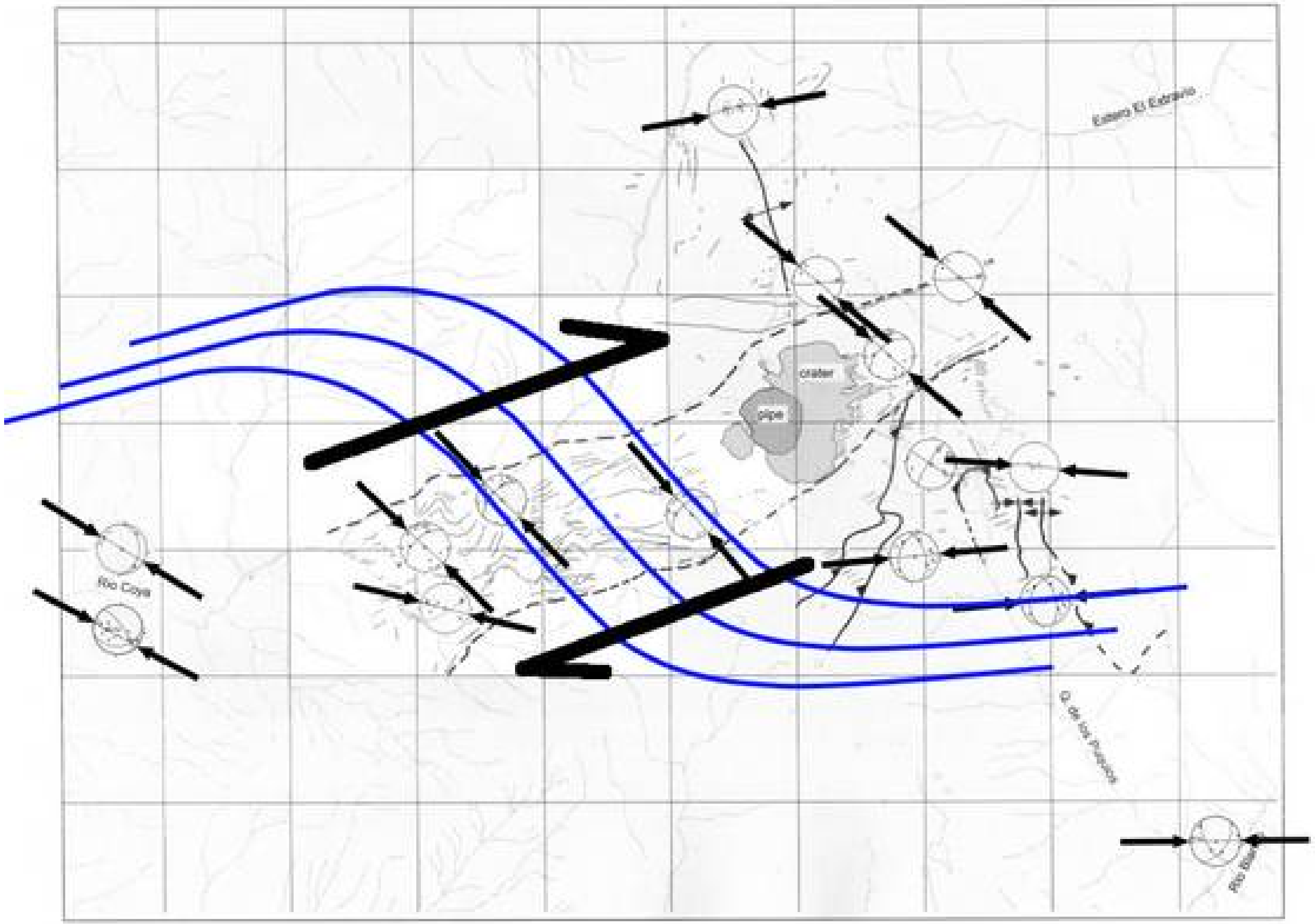

Figure 60: Stress rotation to explain the regional stress at El Teniente?

Figure 61: Mining induced faulting – Green Bar, Tauona mine

Figure 62: No imagine the same fabric on a different scale.

9 What about locked in stress?

Rock is a wonderful material. If you want it to be elastic, it will behave. That is why we can do quick and easy BE modelling which has had a major impact on mine design. When you want it to flow, give it to a geologist and give him TIME. Time is the key word. Similar to old men like me, rock does not have a good memory, over time it forgets. We can even measure its relaxation time (Figure 63). So if you measure anomalous stress, it is not because of “locked in stress” from millions of years ago, but because of local perturbations of the neo-tectonic load.

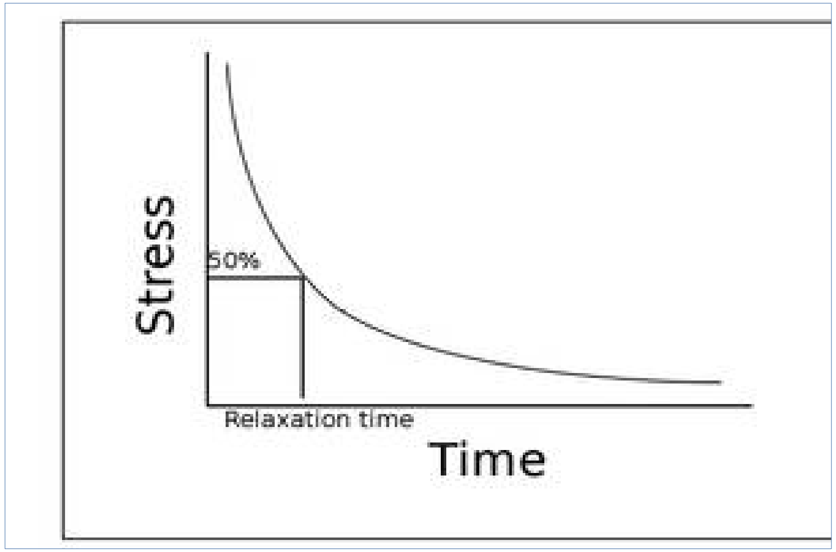

Figure 63: Hiroshi is compressing a cube of strong igneous rock in Prof. Ishi's laboratory and the measuring instrument is showing the elastic response. If Hiroshi could keep the same load for say 100 years, the elastic strain relax because the rock is not perfectly elastic.

10 References

Aben, F., Doan, M.-L., Mitchell, T., Toussaint, R., Reuschlé, T., Fondriest, M., Gratier, J,-P. and Renard, F. (2016). Dynamic fracturing by successive coseismic loadings leads to pulverization in active fault zones. *Journal of Geophysical Research : Solid Earth, American Geophysical Union, 2016, 121, pp.23.*

Adams, G.R., Jager, A.J. and Roering, C. (1981). Investigations of rock fractures around deep level gold mine stopes in H.S. Einstein (comp.)*, Proc. 22nd U.S. Symp.on Rock Mech., Cambridge, MA, 1981. pp. 227–236.*

Bahat, D., Bankwitz, P., Bankwitz, E., Bialik, O and Weinberger, R. (2012). Comparative tectonofractography: fracturing in 19 jointing provinces, experimental results, fracture mechanics considerations and province classification. Z. dt. Ges. Geowiss., 163/4, pp 345–359.

Baird, A.F., McKinnon, S.D. and Godin, L. (2009) Stress channelling and partitioning of seismicity in the Charlevoix seismic zone, Québec, Canada. Geophys. J. Int. Volume 179, 559–568. doi: 10.1111/j.1365-246X.2009.04275.x

Gudmundsson, A., Simmenes, T.H., Larsenb, B. and Philipp, S.L. (2010). Effects of internal structure and local stresses on fracture propagation, deflection, and arrest in fault zones. *Journal of Structural Geology 32(11):1643-1655*

Haschke, M., Jacobson, L.,Van der Westhuizen and Stenekamp, J. (2008) Recent Flexural Slip and Rift-Branch Propagation into the Bushveld Complex, South Africa. *American Geophysical Union, Fall Meeting 2008, Abstract #T43C-2034*

Lenhardt, W.A. and Hagan, T. (1990). Observations and possible mechanism of pillar-associated seismicity at great depth. *Technical Challenges in Deep Level Mining. SAIMM. Johannesburg 1990.*

Ortlepp W.D. (1997). Rock Fracture and Rockbursts - an illustrative study. *SAIMM, Monograph Series M9.*

Pérez-López, R., Paredes, C. and Muñoz-Martín, A. (2005) Relationship between the fractal dimension anisotropy of the spatial faults distribution and the paleostress fields on a Variscan granitic massif (Central Spain): The F-parameter. *Journal of Structural Geology 27(4):663-677*

Perritt, S and Roberts, M. (2007) Flexural slip structures in the Bushveld Complex, South Africa? J. Struct. Geol., Volume 29, 1422-1429.

Pollard, D.D., Segall, P. and Delaney, P.T. (1982). Formation and interpretation of dilatant echelon cracks. *GSA Bulletin (1982) 93 (12): 1291–1303.*

Ramsay, J.G. (1976). Folding and Fracturing of Rocks. *McGraw-Hill, 568p*.

Ramsay, J.G. and Huber, M.I. (1983). *The Techniques of Modern Structural Geology: Strain Analysis*. Academic Press, New York. 307 pp.

Ramsey, J.M. and Chester, F.M. (2004) Hybrid fracture and the transition from extension fracture to shear fracture. NATURE , **428,** pp 64-66.

Reches, Z., and Dewers, T.A. (2005). Gouge formation by dynamic pulverization during earthquake rupture*. Earth Planet. Sci. Lett., 235(1-2), 361–374, doi:10.1016/j.epsl.2005.04.009.*

Reimold, W.U. (2012) Comment on ”Pseudotachylite in the south Boundary Fault at the Cooke shaft, Witwatersrand Basin, South Africa by P.W. Mambane et al.*, South African Journal Of Geology 114.2, 109-120. Downloaded from http://pubs.geoscienceworld.org/gssa/sajg/article-pdf/115/2/251/2964733/251_Reimold.pdf.*

Sagy, A., Fineberg, J. and Reches, Z. (2004) Shatter cones: branched, rapid fractures formed by shock impact*. Journal of Geophysical Research, Vol. 109, B10209, Doi:10.1029/2004jb003016, 2004*

Shand, S.J. (1916). The pseudotachylite of Parys (Orange Free State), and its relation to 'Trap-shotten gneiss' and 'flinty crush-rock'. *Q. 1. geol. Soc. Lond., 72,198-217*

Sharon, E., G. Cohen, and J. Fineberg (2002), Crack front waves and the dynamics of a rapidly moving crack. *Physical Review Letters, 88 (8).*

Stacey, T.R. (1981). A simple extension strain criterion for fracture of brittle rock. *Int. J. Rock Mech. Min. Sci. & Geomech. Abstr. Vol. 18. pp. 469 to 474.*

Steenekamp, J.M.A., van der Westhuizen, W.A., Bateman, M.D., Jacobson, L and Nel, L. (2018) A Pleistocene Thrust Fault in Anorthosite of the Rustenburg Layered Suite near Mooinooi, North West Province, South Africa: Neotectonic Implications. *South African Journal of Geology,Volume 121.4, Page 421-430. Doi:10.25131/ Sajg.121.0033*

Therriault, A.M., Grieve, R.A.' and. Reimold, W. U (1997) Original size of the Vredefort Structure: Implications for the geological evolution of the Witwatersrand Basin. *Meteoritcs & Planetary Science 32,71-77.*

van Aswegen, G. and Stander, M. (2012) Origins of some fractures around tabular stopes in deep South African mines, *J. S. Afr. Inst. Min. Metall., vol. 112, pp 729-734.*